Effects of Prenatal Exposure to Folate Metabolism Antagonist, Methotrexate on Placenta and Fetal Brain in Rats

葉酸代謝拮抗剤 Methotrexate のラット妊娠期曝露が胎盤および胎児脳へ及ぼす影響

The United Graduate School of Veterinary Science

Yamaguchi University

Jing SUN

March 2014

CONTENTS

GENERAL INTRODUCTION

The folate metabolism antagonist, methotrexate (MTX), a structural analog of folic acids, inhibits dihydrofolate reductase that reduces dihydrofolate to tetrahydrofolate. MTX therefore limits the availability of one-carbon fragments necessary for the synthesis of purines, and interferes with the conversion of deoxyuridylate to thymidylate in the synthesis of DNA (Lloyd et al., 1999; Genestier et al., 2000; Hyoun et al., 2012). This results in MTX-mediated inhibition of cell proliferation, disruption of cell cycle and induction of apoptosis in susceptible cells (Genestier et al., 2000). MTX has historically been used as an antineoplastic agent (Wright et al., 1951) but has had a broader role in several areas of medicine in the past 2 decades (Kremer and Phelps, 1992; Kumar et al., 1994). More recently, it has been used in the treatment of gestational trophoblast disease, and autoimmune diseases such as rheumatoid arthritis, systemic lupus erythematosus, Crohn's disease, psoriasis, and psoriatic arthritis (Cuellar and Espinoza, 1997; DeLoia et al., 1998; Genestier et al., 2000; Cronstein, 2005). MTX is also used as an abortifacient, both for the voluntary termination of pregnancy and for the medical management of ectopic pregnancy (Kozma and Ramasethu, 2011).

In humans, maternal exposure to MTX during critical periods of

embryogenesis induces miscarriages and embryopathy (Del Campo et al., 1999; Martinez et al., 2009). The previous case reports in human showed that embryopathy such as nervous system anomalies, growth retardation, craniofacial deformities and skeletal defects, resulted from failed attempts at termination of pregnancy with MTX or when mothers who are taking MTX for medical reasons become pregnant inadvertently (Bawle et al., 1998; Lloyd et al., 1999; Seidahmed et al., 2006; Corona-Rivera et al., 2010; Hyoun et al., 2012). In experimental animals, prenatal MTX exposure reportedly induced resorption, intrauterine death, hypotrophy or congenital malformations in rats, mice and rabbits (Skalko and Gold, 1974; Tsibangu et al., 1975; Jordan et al., 1977), and slight embryolethality in rhesus monkeys (Wilson et al., 1979). However, despite the fact that the placenta is one of the important organs for evaluation of risks for the dam and embryo, few researchers have sufficiently focused on the detailed histopathological findings of the placenta exposed to MTX to date.

As for the brain anomalies in MTX-induced embryopathy in humans, clinical findings of alobar/semilobar holoprosencephaly (Seidahmed et al., 2006; Corona-Rivera et al., 2010), cerebellar hypoplasia (Seidahmed et al., 2006), agenesis of the corpus callosum (Seidahmed et al., 2006) and microcephaly (Bawle et al., 1998;

Garcia-Minaur and Botella, 2000) have been reported. Moreover, prenatal MTX exposure reportedly induced a decrease in net weights of the brain in chicken, and hydrocephalus in rabbits. Nevertheless, detailed histopathological findings and pathogenesis of MTX-induced brain anomalies in fetus of human and experimental animals remain unclear.

The present studies were carried out to clarify the toxic effects of prenatal MTX administration on the placenta and fetal brain. In chapter 1, we performed the sequential histopathological examinations in the placenta after exposure to MTX in pregnant rats. In chapter 2, we examined histopathologically the time-dependent changes of fetal brain following MTX administration to their dams. The purpose of the present study is to elucidate the pathogenesis of the damage of placenta and fetal brain induced by MTX.

CHAPTER 1

Effect of Methotrexate on Rat Placenta Development

1.1 Introduction

The placenta is an interface between the dams and the embryos/fetuses, and is a multifaceted organ that performs a number of essential and significant functions that are modified during gestation. These include anchoring the developing fetus to the uterine wall, mediating maternal immune tolerance, and maintaining O_2/CO_2 exchange and nutrient/metabolite requirements during embryonic development (Bauer et al., 1998; Furukawa et al., 2011). It also functions as a barrier protecting embryos/fetuses from xenobiotics, and releases a variety of steroids, hormones and cytokines (Furukawa et al., 2011). Thus, the growth and function of the placenta play important roles in the maintenance of pregnancy, and influences fetal development. The placenta is a target organ highly susceptible to drug- or chemical material-induced adverse effects (Furukawa et al., 2011). Drug- or chemical material-induced placental functional disorders result in developmental abnormality of the fetus (Furukawa et al., 2011). Thus, the placenta is an important organ for evaluating embryonic developmental toxicity and understanding its mechanism.

Folates function in various one-carbon transfer reactions, including purine and thymidylate biosynthesis, amino acid metabolism, and formate oxidation (Wagner, 1995). Purine and thymidylate biosynthesis is a fundamental requisite event

underlying DNA and RNA synthesis (Tamura and Picciano, 2006). These folate-dependent reactions are essential for fetal development and maternal well-being (Tamura and Picciano, 2006). Folic acid may also have important roles in other physiological pathways needed for successful pregnancy, including angiogenesis (Sasaki et al., 2003; Williams et al., 2011), methylation of the homocysteine (Ciaccio et al., 2008), antioxidant effect (Joshi et al., 2001), and endothelial-dependent vascular relaxation (Griffith et al., 2005). These processes are essential for the establishment of fetoplacental circulation. However, little is known about histopathological changes in placentas induced by folate metabolism impairment or folate deficiency.

Folate metabolism antagonist, methotrexate (MTX), a structural analog of folic acids, inhibits the reduction of dihydrofolate to tetrahydrofolate, resulting in the inhibition of DNA and RNA synthesis (Margolis et al., 1971; Jolivet et al., 1983). This results in MTX-mediated inhibition of cell proliferation, disruption of cell cycle and induction of apoptosis in susceptible cells (Genestier et al., 2000). MTX has been used in the treatment of neoplastic diseases, gestational trophoblast disease, and autoimmune diseases such as rheumatoid arthritis, systemic lupus erythematosus, Crohn's disease, psoriasis, and psoriatic arthritis (Cuellar and Espinoza, 1997; DeLoia et al., 1998; Genestier et al., 2000). MTX is also used in the medical management of

ectopic pregnancy and for medical termination of pregnancy (Creinin and Krohn, 1997; Lipscomb, 2007). In humans, maternal exposure to MTX during pregnancy induces miscarriages, neonatal malformations and developmental delays (Del Campo et al., 1999; Martinez Lopez et al., 2009). MTX is embryotoxic and teratogenic in rats, mice and rabbits (Skalko and Gold, 1974; Tsibangu et al., 1975; Jordan et al., 1977), and is abortifacient in rhesus monkeys (Wilson et al., 1979). However, there have been few reports on the detailed histopathological findings of the placenta exposed to MTX, and it remains unclear how placental pathology might affect fetal growth. In the present study, we investigated the sequential histopathological changes in the placenta after exposure to MTX in pregnant rats to clarify the role of the placenta in the induction of fetal developmental disability induced by folate metabolism antagonist, MTX.

1.2 Materials and methods

1.2.1 Animals

All experiments were performed using female Wistar Imamichi rats, 9 weeks of age, 223.66 ± 1.69 g (mean ± SE) in weight and obtained from the Institute of Animal Reproduction (Ibaraki, Japan). The animals were reared in a room with the

temperature controlled at 22 ± 2 ˚C, humidity at 50 ± 5%, with ventilation 11 times per hour and lighting set at 12:12-h light/dark cycle (light cycle, 7:00-19:00), and they were given standard chow (CE-2; Nihon Clea, Tokyo, Japan). The present experiments were performed following the provisions approved by the Animal Research Committee of Tottori University.

1.2.2 Experimental design

Day 0 of gestation (GD 0) was designated as the day when the presence of a vaginal plug was identified. A total of 44 animals were divided into three different groups as follows: (1) saline-treated control rats (n = 16), (2) MTX-GDs 11 and 12-treated rats (n = 16), (3) MTX-GDs 13 and 14-treated rats (n = 12). MTX (Pfizer Japan Inc., Tokyo, Japan) was dissolved in saline and administered intraperitoneally. The rats received intraperitoneal injections (i.p.) with MTX (0.2 mg/kg body weight) or saline (the control) during GDs 11-12 or GDs 13-14. The dose level in the present study was previously reported to induce an impairment of the fetus in rats (Jordan et al., 1977; Wilson et al., 1979). The specific timing of MTX administration was selected because the glycogen cells, which constitute one of the important elements in the basal zone, are detected from GD 11 (Peel and Bulmer, 1977). Maternal body

weight was recorded on GDs 0-21. Placenta and fetus samples were collected under pentobarbital anesthesia (100 mg/kg, i.p.) on GDs 13 (except for the GD13,14-treated group), 15, 17 and 21. All embryos/fetuses were removed from the placentas. Half of the placentas were separated between the basal zone and decidua basalis, removed from the uterine wall, and weighed. The embryos/fetuses and removed placentas were weighed. The fetuses on GD21 were macroscopically examined for external malformations. All procedures were conducted between 9 and 11 a.m.

1.2.3 Histopathological examination of rat placentas

All placentas were fixed in 10% neutral buffered formalin. These tissues were embedded in paraffin, sectioned 4 μm in thickness, and stained with hematoxylin and eosin (HE). The thickness of the labyrinth zone, basal zone, decidua basalis and metrial gland close to the central portion were measured in placentas from each dam with histomorphometric analysis software (Olympus Corporation, Tokyo, Japan).

1.2.4 Immunohistochemical examinations of rat placentas

For immunohistochemistry, mouse monoclonal antibodies for Phospho-Histone H3 (Epitomics, Inc., CA, USA) were used as the primary antibodies.

All sections were dewaxed, rehydrated, rinsed with 0.05 M Tris-buffered saline (TBS; pH 7.6), treated with 3% hydrogen peroxide, and then rinsed again with TBS. Tissue sections for detection of both antigens were immersed in 0.01 M citrate buffer (pH 6.0/Dako, Glostrup, Denmark) and autoclaved for 15 min at 121 ˚C to retrieve the antigens. Slides were incubated with the primary antibody (1:300 dilution) for 30 min at room temperature, rinsed with TBS, and treated with Simple Stain MAX-PO (Nichirei, Tokyo, Japan) for 30 min at room temperature. They were then rinsed with TBS before being treated with a 3,3'-diaminobenzidine solution containing 0.01% hydrogen peroxide to facilitate a peroxidase color reaction. After a further wash with TBS, the slides were counterstained with Mayer's hematoxylin.

Apoptotic bodies in the placenta were detected by terminal deoxynucleotidyl-transferase (TdT)-mediated deoxyuridine triphosphate-digoxigenin (dUTP) nick-end labeling (TUNEL), which was performed using an *in situ* apoptosis detection kit (Trevigen, Inc., Gaithersburg, MD, USA). The criteria of apoptosis included TUNEL staining and the presence of pyknotic nuclei. The number of TUNEL or Phospho-Histone H3-positive cells was counted in ten different fields in the labyrinth and the basal zones by light microscopy with a 20× objective lens, and with above-mentioned histomorphometric analysis software.

1.2.5 Statistical analysis

All data were expressed as means ± standard error (SE) in each group. The results in each group were compared by Student's *t*-test or Dunnett's multiple comparison test with statistical software (SSRI Co., Ltd., Tokyo, Japan). $P < 0.05$ or $P < 0.01$ was considered to be statistically significant.

1.3 Results

1.3.1 Effects on dams

Body weight gains of dams decreased significantly during GDs 13-21 in the GD11,12-treated group compared with the control group, whereas in the GD13,14-treated group, significant declining body weight gains of dams were not observed throughout the experimental period compared with the control group (Fig. 1). However, dams neither in the control nor the two MTX-treated groups showed any other clinical signs during the experimental period.

1.3.2 Effects on embryos/fetuses and placentas

In the GD11,12-treated group, the number of living fetuses per litter tended to decrease and the fetal mortality rates tended to increase throughout the experimental

period (Table 1). The fetal weights were significantly reduced on GD 13 and the placen-tal weights were significantly reduced on GDs 13 and 15 in the GD11,12-treated group (Table 1). The placentas on GD 17 were macroscopically small (Fig. 2). In the GD11,12-treated group, no macroscopic fetal abnormalities were observed in the external examination on GD21. No significant macroscopical changes were detected in placentas and fetuses of the GD13,14-treated group.

1.3.3 Histopathological findings of placentas

In the GD11,12-treated group, a marked thinning of basal zone was detected on GD13 and this significant pathological change was continued throughout the experimental period, whereas the thickness of the labyrinth zone decreased significantly during GDs 13-17 (Figs. 3 and 4). The severity of thinning of the basal zone was higher than that of the labyrinth zone (Figs. 3 and 4). In the basal zone of the GD11,12-treated group, there were significant decreases in both spongiotrophoblasts and trophoblastic giant cells on GD13, compared with those of the control group (Fig. 4c and d). In addition, a significant decrease in mitotic cells and Phospho-Histone H3-positive cells was detected in basal zone of GD11,12-treated group on GD13, compared with the control group (Figs. 4, 6 and 7). Apoptotic cells,

which were characterized by pyknosis or karyorrhexis, phagocytosis and cell debris, and positively stained by the TUNEL method, increased significantly on GD 13 in the basal zone of the GD11,12-treated group (Figs. 4, 6 and 7). There were no significant differences in the number of Phospho-Histone H3-positive cells and TUNEL-positive cells in the labyrinth zone between the control group and the GD11,12-treated group throughout the experimental period (Fig. 7). A marked decrease in glycogen cell-islands in the basal zone was detected, and there was a reduction in the interstitial invasion of glycogen cell-like trophoblasts into the metrial gland on GD 15 in the GD11,12-treated group (Fig. 5). No significant histopathological changes in the decidua basalis and metrial gland were noted throughout the experimental period in the GD11,12-treated group. In the GD13,14-treated group, there were no other significant histopathological changes in the placentas than thinning of the labyrinth zone on GD 17.

1.4 Discussion

In the present study, the administration of MTX at 0.2 mg/kg/day during GDs 11-12 induced a significant thinning of the basal zone during the experimental period, and the labyrinth zone only on GDs 13, 15 and 17. The severity of thinning of the

basal zone was higher than that of the labyrinth zone. In the GD11,12-treated group, a significant decrease of cell proliferation marker, Phospho-Histone H3-positive cells, and a major increase in apoptotic marker, TUNEL-positive cells, were detected on GD13 in the basal zone. By contrast, in the GD13,14-treated group, there were no other significant changes in placentas and fetuses throughout the experimental period than thinning of the labyrinth zone on GD 17. These results indicated that component cells in the basal and labyrinth zones on GDs 11-12 are more highly sensitive to MTX than those of GDs 13-14.

In normal rat placentas of GDs 11-21, a cell proliferation marker, PCNA expression in trophoblasts, fetal vessel endothelial cells of the labyrinth zone, and spongiotrophoblasts of the basal zone were highest on GD 11 and 13, and decreased as pregnancy progressed (Acar et al., 2008). These results showed that trophoblasts and spongiotrophoblasts on GDs 11-12 have higher cell-proliferative activity than those of GDs 13-14. This is related to the higher sensitivity to MTX of their component cells in the basal and labyrinth zones of GDs 11-12 than those of GDs 13-14. In normal human placentas, PCNA expression in cytotrophoblasts is highest in the very early term of pregnancy and significantly decreases with the advance of pregnancy (Ishihara et al., 2000). It is speculated that the toxic effects of MTX on

placental development are diminished with the advance of pregnancy after mid-gestation.

In the present study, MTX exposure on GDs 11-12 induced not only labyrinth zone hypoplasia during GDs 13-17 but also severe hypoplasia of basal zone throughout the experimental period. The hypoplasia of the basal zone was more severe than that of the labyrinth zone. Although there were few reports describing detailed histopathological findings of placental lesions induced by anti-cancer drugs, the effects of cisplatin or 6-mercaptopurine on rat placental development have been previously studied (Furukawa et al., 2008, 2013). In the previous study, cisplatin exposure on GDs 11-12 induced severe hypoplasia in both the labyrinth basal zones (Furukawa et al., 2013) and 6-mercaptopurine exposure on GDs 11-12 induced more severe hypoplasia of the labyrinth zone than that of the basal zone (Furukawa et al., 2008). These results may suggest that it is possible that MTX affects the component cells in the basal zone of GDs 11-12 more strongly than those in the labyrinth zone of GDs 11-12, compared with cisplatin or 6- mercaptopurine. Additionally, from a result of the present study, it is hypothesized that folate metabolism is carried out more actively in the basal zone of GDs 11-12 than labyrinth zone of GDs 11-12. Recent study demonstrated that folic acid has important roles in physiological pathways

needed for placental development including extravillous trophoblast invasion, angiogenesis, and secretion of MMPs (Williams et al., 2011). The risks of placenta-mediated adverse outcome such as preeclampsia and placental abruption were greater for women exposed to folic acid antagonists during pregnancy than women without such exposure (Wen et al., 2008). However, little attention has been given to the developmental stage and site of the placenta strongly affected by folate metabolism impairment or folate deficiency have been clarified. This is the first study demonstrating that the basal zone is strongly affected by folate metabolism antagonist. These results can be useful in order to prevent the occurrence of a placenta-mediated adverse outcome induced by folate metabolism impairment and folate deficiency.

The basal zone is comprised of three differentiated cell types: (1) spongiotrophoblasts, (2) trophoblastic giant cells and (3) glycogen cells (Ain et al., 2003). The trophoblastic giant cells are analogous to human extravillous cytotrophoblast cells and located at the maternal-placental interface (Soares et al., 1996). These cells stop dividing and continue to replicate DNA (endoreduplication) to become polyploidy (Soares et al., 1996; Watson and Cross, 2005). The spongiotrophoblasts directly originate from the ectoplacental cone and are located immediately above the trophoblastic giant cell layer. Although spongiotrophoblasts

are morphologically distinct from trophoblast giant cells, both of them exhibit endocrine activities (Soares et al., 1996). Glycogen cells are characterized by a vacuolated glycogen-rich cytoplasm and appear as compact cell islets (Davies and Glasser, 1968; Bouillot et al., 2006). Glycogen cells are detected in the spongiotrophoblasts layer in mid-gestation, and disappear at the end of pregnancy (Davies and Glasser, 1968). The trophoblasts originated from the glycogen cells invade the decidua and metrial gland (Furukawa et al., 2011). The spongiotrophoblasts and trophoblastic giant cells in the basal zone produce a prolactin-like hormone with lactogens and cytokines during pregnancy to maintain progesterone secretion from the corpus luteum (Ain et al., 2003; Malassiné et al., 2003; Soares, 2004). It has been suggested that another function of the basal zone is to limit the growth of maternal endothelium into the fetal placenta (Coan et al., 2006). Spongiotrophoblasts produce anti-angiogenic proteins such as Flt1 (an antagonist of VEGF) and Prp (an antagonist of Plf) (He et al., 1999). Although their initial appearance within the spongiotrophoblast layer and their expression of spongiotrophoblast-specific genes imply that glycogen cells are a specialized subtype of spongiotrophoblast cell (Adamson et al., 2002), the developmental origin of glycogen cells is not entirely clear. Although the functions of glycogen cells have

been unclear, it is speculated that they are related with glycogen metabolism because glucagons are detected in glycogen cells (Coan et al., 2006). It is possible that the decrease in the number of living fetuses per litter and the increase of fetal mortality in the present study are related to a decrease in spongiotrophoblasts and glycogen cells; namely, basal zone hypoplasia. After this study, it is expected that a clarification of the relation between basal zone hypoplasia and abnormal fetal development will take place.

In conclusion, MTX administration at 0.2 mg/kg/day during GDs 11-12 induced developmental retardation of the basal and labyrinth zones, leading to small placentas, though MTX treatment during GDs 13-14 induced few pathological changes in the placenta. The severity of developmental retardation of the basal zone induced by MTX exposure during GDs 11-12 was higher than that of the labyrinth zone. It is considered that the component cells of the basal and labyrinth zones on GDs 11-12 are more highly sensitive to MTX than those on GDs 13-14 and that the component cells of the basal zone are more sensitive to MTX than those of the labyrinth zone. To our knowledge, this is the first report demonstrating histopathological findings of placental developmental retardation induced by MTX.

Table 1. Effects of methotrexate on fetuses and placentas

Autopsy	Treatment	Day of treatment	No. of dams	Total No. of live fetuses	Living fetuses per litter	Fetal mortality (%)	Fetal weight (g)	Placental weight (g)
GD13	Control	-	4	66	16.50 ± 1.04	4.53 ± 2.97	0.070 ± 0.004	0.096 ± 0.006
	MTX	11, 12	4	49	12.25 ± 1.89	25.48 ± 11.74	0.054 ± 0.003*	0.083 ± 0.013*
GD15	Control	-	4	63	15.75 ± 0.48	0.00 ± 0.00	0.267 ± 0.008	0.215 ± 0.011
	MTX	11, 12	4	36	9.00 ± 2.04‡	30.28 ± 9.64‡	0.252 ± 0.010	0.163 ± 0.013‡
		13, 14	4	59	14.75 ± 0.63	2.94 ± 2.94	0.250 ± 0.010	0.220 ± 0.010
GD17	Control	-	4	58	14.50 ± 1.56	2.08 ± 2.08	0.815 ± 0.009	0.319 ± 0.005
	MTX	11, 12	4	47	11.75 ± 2.17	22.38 ± 12.94	0.842 ± 0.015	0.259 ± 0.026
		13, 14	4	55	13.75 ± 1.03	5.42 ± 1.85	0.820 ± 0.013	0.284 ± 0.031
GD21	Control	-	4	68	17.00 ± 0.71	1.39 ± 1.39	5.000 ± 0.050	0.447 ± 0.013
	MTX	11, 12	4	39	9.75 ± 2.21‡	11.39 ± 4.98†	5.217 ± 0.074	0.472 ± 0.015
		13, 14	4	64	16.00 ± 0.91	0.00 ± 0.00	5.071 ± 0.140	0.432 ± 0.011

Values are expressed as means ± SE.

*: P<0.05, compared with control (Student's *t*-test).

†: P<0.05, compared with control (Dunnett's multiple comparison test).

‡: P<0.01, compared with control (Dunnett's multiple comparison test).

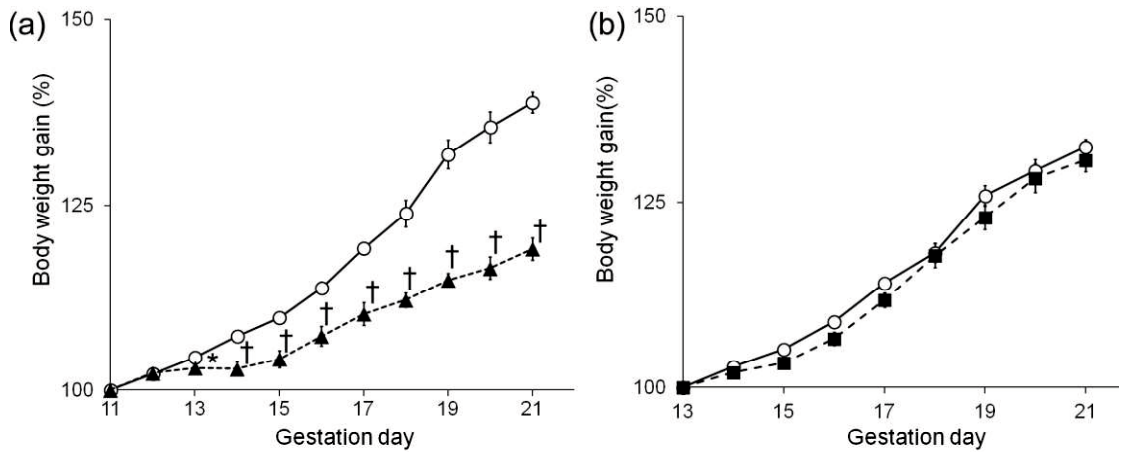

Fig. 1 Body weight gains of dams decreased significantly during GDs 13-21 in the GD11,12-treated group compared with the control group (a), whereas in the GD13,14-treated group, significant declining body weight gains of dams were not observed throughout the experimental period compared with the control group (b). ○: Control. ▲: GD11,12-treated group. ■: GD13,14-treated group. Values are expressed as means ± SE. *: $P<0.05$, compared with control (Student's *t*-test); †: $P<0.01$, compared with control (Student's *t*-test).

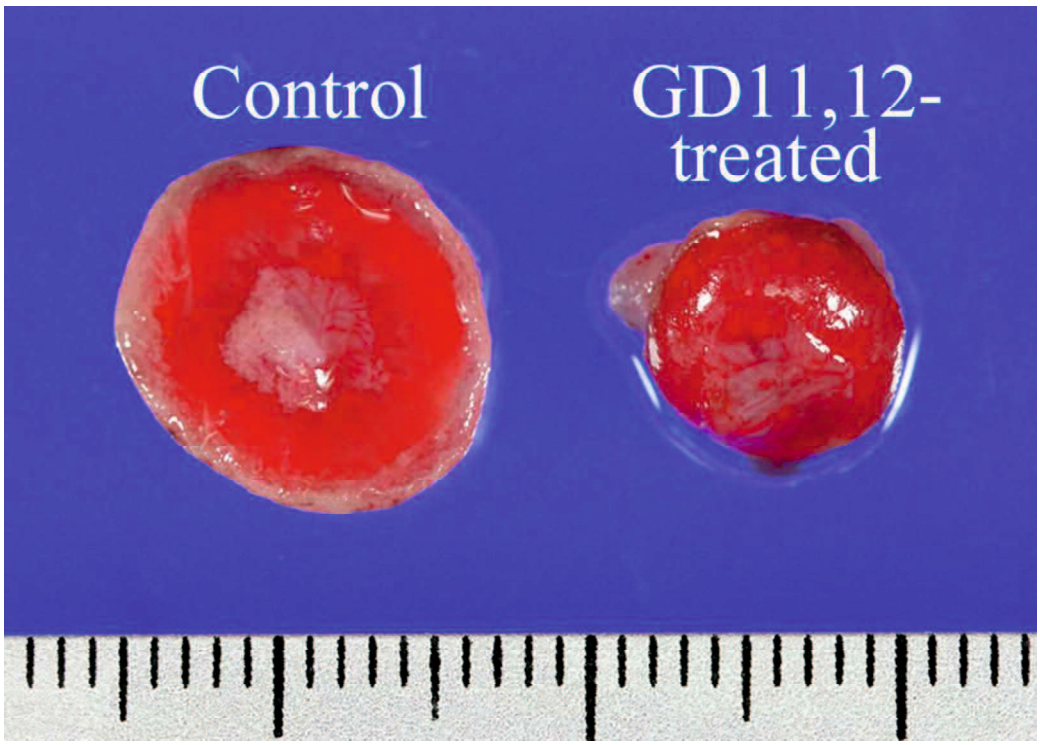

Fig. 2. Gross appearance of placenta on GD17 of the control (left) and the GD11,12-treated group (right). The placenta in GD11,12-treated group was macroscopically smaller than that of control. The ruler in the figure is graduated in millimeters.

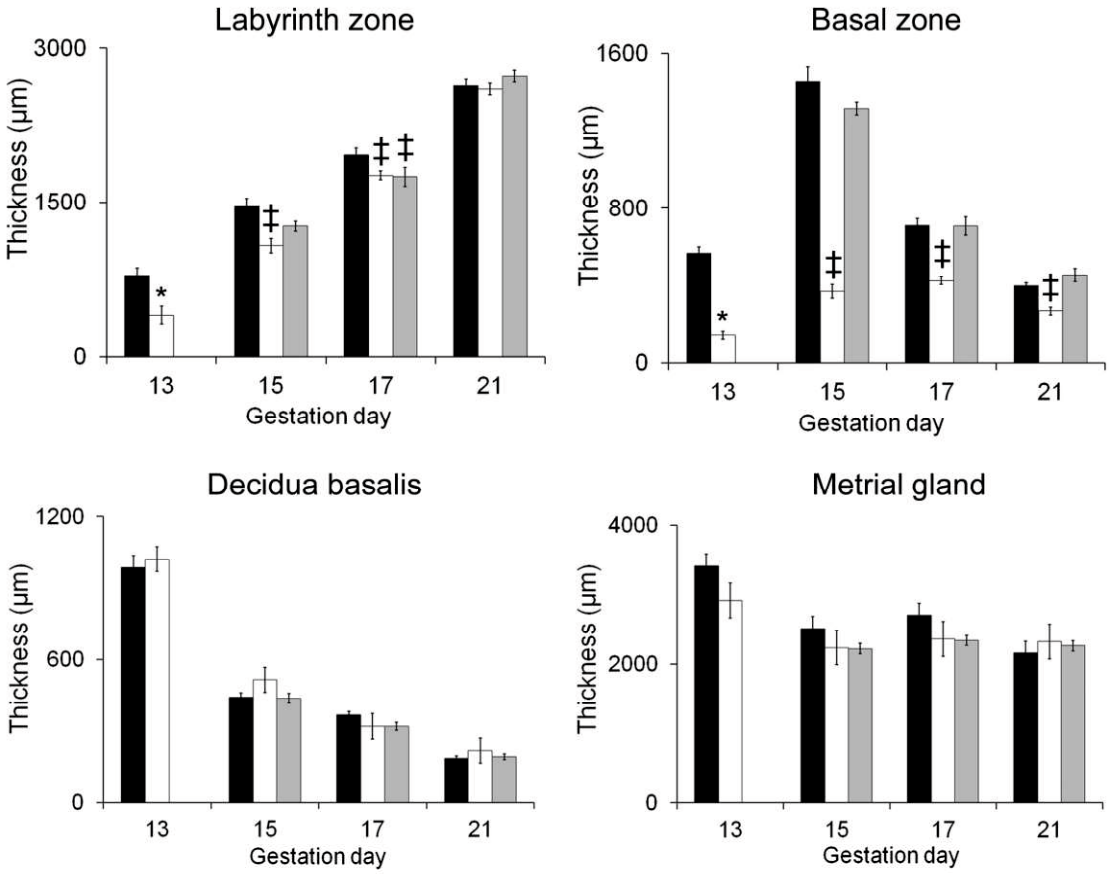

Fig. 3. Thickness of the labyrinth zone, basal zone, decidua basalis and metrial gland. ■: Control. □: GD11,12-treated group. ■: GD13,14-treated group. Values are expressed as means ± SE. *: P<0.01, compared with control (Student's *t*-test); †: P<0.05, compared with control (Dunnett's multiple comparison test); ‡: P<0.01, compared with control (Dunnett's multiple comparison test).

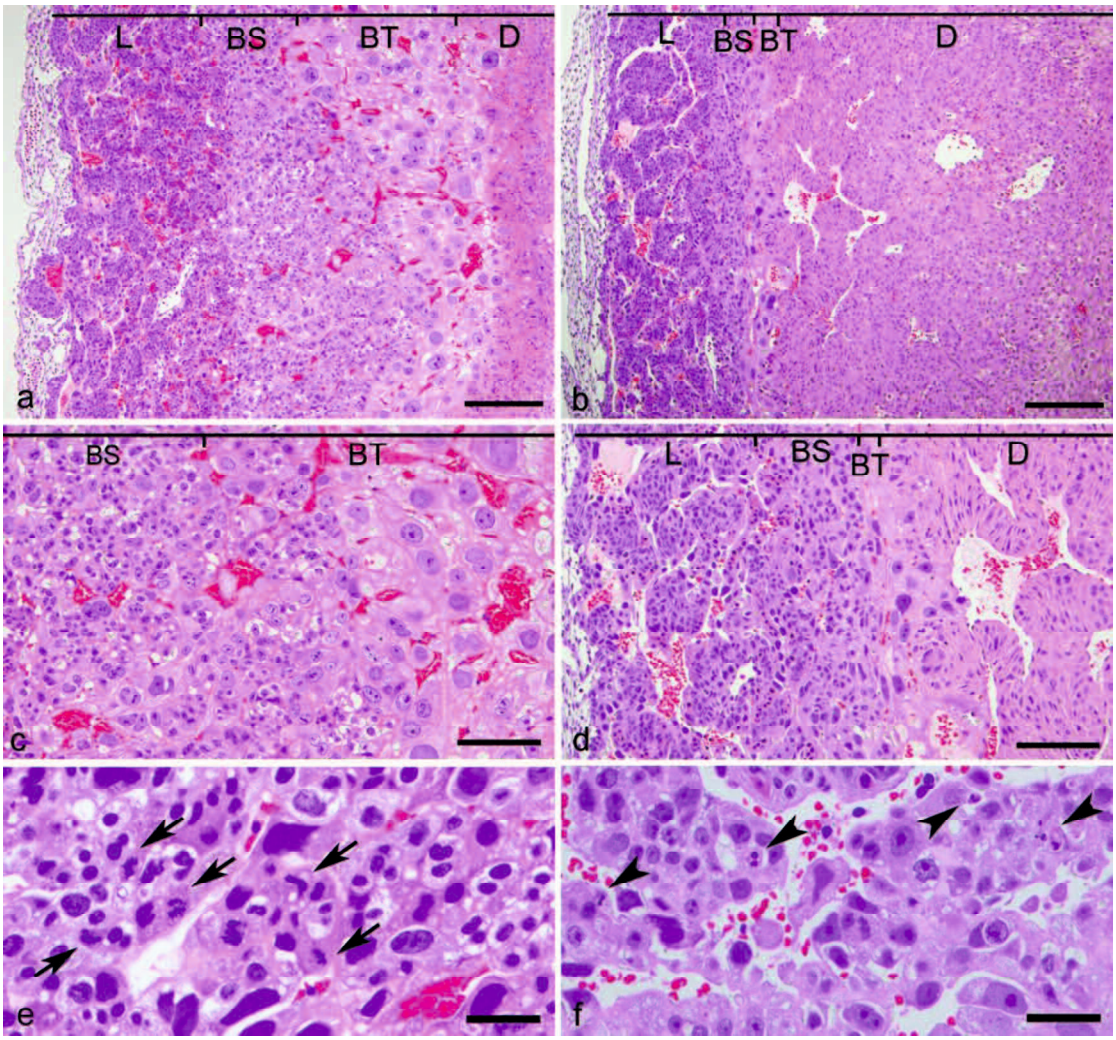

Fig. 4. Histopathological findings of placentas on GD13 of control (a, c and e) and GD11,12-treated group (b, d and f). (L) Labyrinth zone, (BS) Basal zone spongiotrophoblast layer, (BT) Basal zone trophoblastic giant cell layer, (D) Decidua basalis. (a and b) Bar=200 μm, (c and d) Bar=100 μm, (e and f) Bar=30 μm. (a) Low power field in control. (b) Low power field in GD11,12-treated group. Marked thinning of basal and labyrinth zones was observed. (c) Basal zone of the control, both spongiotrophoblasts and trophoblastic giant cells were observed. (d) In the basal zone of the GD11,12-treated group, both spongiotrophoblasts and trophoblastic giant cells were significantly diminished. (e) High power field in the basal zone of control. Arrows show mitosis. (f) High power field in the basal zone of GD11,12-treated group. Arrowheads show apoptotic cells, characterized by pyknosis or karyorrhexis.

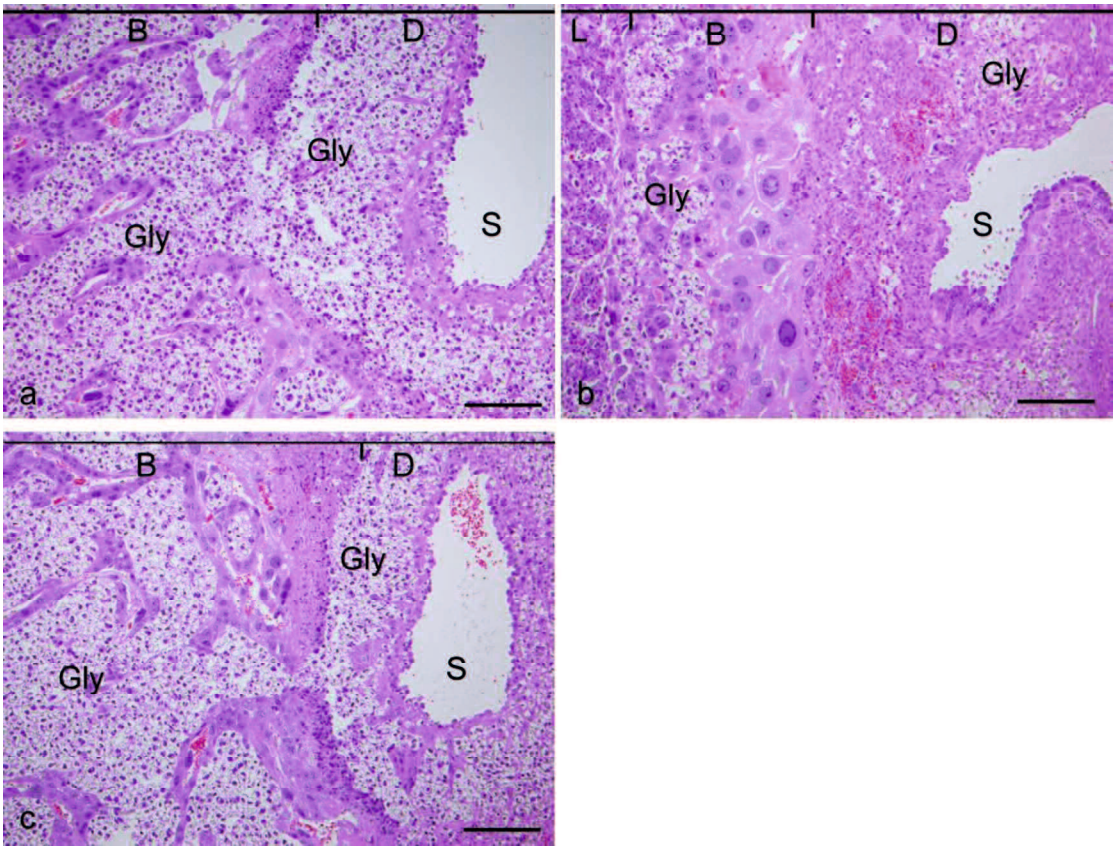

Fig. 5. Histopathological findings of placentas on GD15. (L) Labyrinth zone, (B) Basal zone, (D) Decidua basalis, (S) Spinal artery, (Gly) Glycogen cell-islands, Glycogen cell-like trophoblasts. Bar=200 μm. (a) Control. (b) GD11,12-treated group. (c) GD13,14-treated group. A marked decrease in glycogen cell-islands and an inhibition of the interstitial invasion of glycogen cell-like trophoblasts into metrial gland were detected in the GD11,12-treated group.

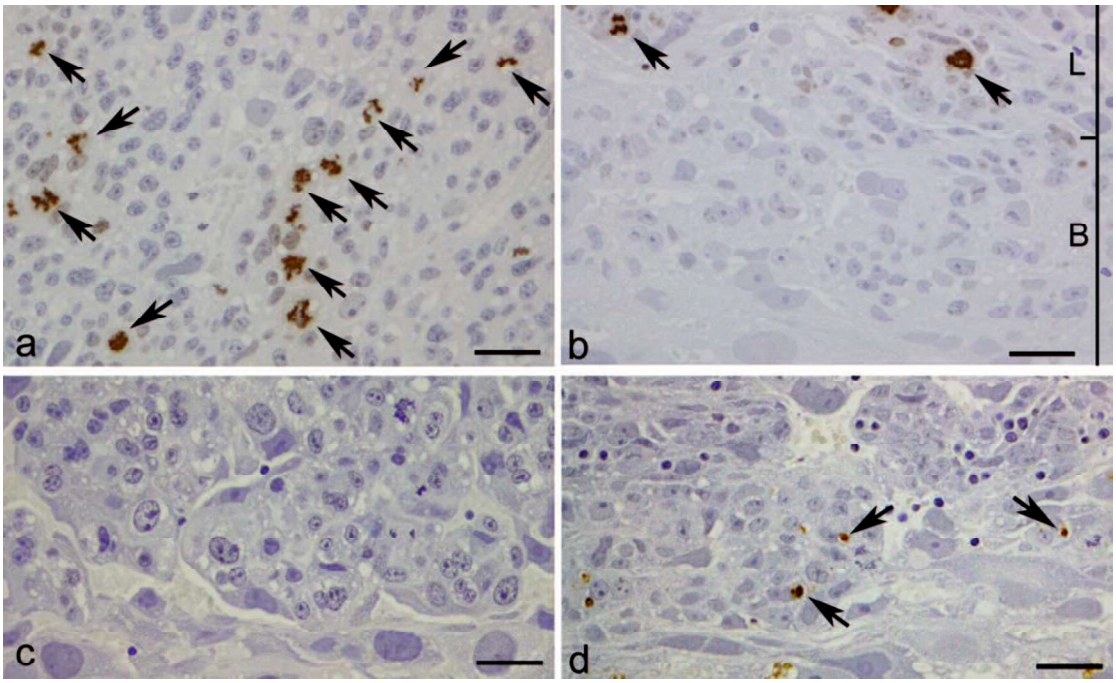

Fig. 6. Immunohistochemical expression of Phospho-Histone H3 (a and b) and TUNEL-positive cells (c and d) in basal zone on GD13. (L) Labyrinth zone, (B) Basal zone. Bar=30 μm. (a and c) Control. (b and d) GD11,12-treated group. In the GD11,12-treated group, there were decreases in Phospho-Histone H3-positive cells and increases in TUNEL-positive cells on GD13.

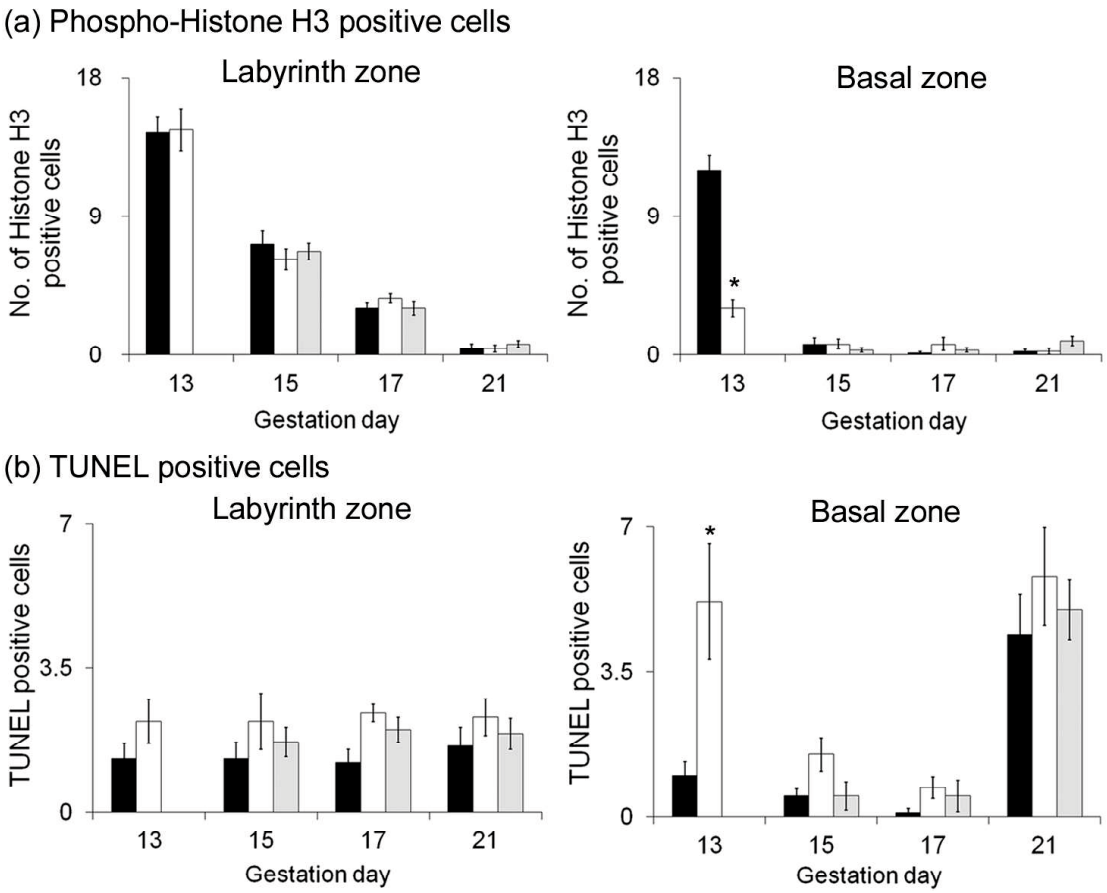

Fig. 7. Number of Phospho-Histone H3-positive cells and TUNEL-positive cells in the labyrinth and basal zones. ■ : Control. □ : GD11,12-treated group. ■ : GD13,14-treated group. Values are expressed as means ± SE. *: P<0.05, compared with control (Student's *t*-test).

CHAPTER 2

Effect of Methotrexate on Neuroepithelium in the Rat Fetal Brain

2.1 Introduction

A folate antagonist, methotrexate (MTX), inhibits dihydrofolate reductase that reduces dihydrofolate to tetrahydrofolate. MTX therefore limits the availability of one-carbon fragments necessary for the synthesis of purines and interferes with the conversion of deoxyuridylate to thymidylate in the synthesis of DNA and cell proliferation (Lloyd et al., 1999; Genestier et al., 2000; Hyoun et al., 2012). MTX is known to induce apoptosis, and the mechanism of MTX-induced apoptosis is considered to be associated with the up-regulation of p53 and p21 proteins (Kobayashi et al., 2002; Spurlock et al., 2012), repression of the induction of c-Jun N-terminal kinase (JNK) activity, expression of the CD95 receptor/ligand system (Müller et al., 1997) and reactive oxygen species (Herman et al., 2005; Spurlock et al., 2012).

MTX has been used in the treatment of malignancy, autoimmune and inflammatory diseases and gestational trophoblast disease (Cuellar and Espinoza, 1997; DeLoia et al., 1998; Genestier et al., 2000). MTX is also used as an abortifacient, both for the voluntary termination of pregnancy and for the medical management of ectopic pregnancy (Kozma and Ramasethu, 2011). Medical treatment protocols for MTX were established in the 1980s and have become a widely accepted

primary treatment for unruptured ectopic pregnancy (Pisarska et al., 1998; Lipscomb, 2007; Practice Committee of American Society for Reproductive Medicine, 2008). In humans, MTX embryopathy results from failed pregnancy termination with MTX or when mothers who are taking MTX for medical reasons become pregnant inadvertently (Bawle et al., 1998; Seidahmed et al., 2006; Corona-Rivera et al., 2010; Hyoun et al., 2012). The anomalies of MTX embryopathy include nervous system anomalies, growth deficiency, craniofacial deformities and skeletal defects (Lloyd et al., 1999; Hyoun et al., 2012). As the central nervous system anomalies in MTX embryopathy, alobar/semilobar holoprosencephaly (Seidahmed et al., 2006; Corona-Rivera et al., 2010), cerebellar hypoplasia (Seidahmed et al., 2006), agenesis of the corpus callosum (Seidahmed et al., 2006) and microcephaly (Bawle et al., 1998; Garcia-Minaur and Botella, 2000) have been reported. However, there are few reports to examine the brain anomalies in MTX embryopathy histopathologically, and their detailed histopathogical findings or their detailed pathogenesis remain unclear. In experimental animals, prenatal MTX exposure reportedly induced anomalies of the brain in chicken (Zamenhof, 1985) and rabbits (Jordan et al., 1977). In rabbit, MTX administration on gestation days (GD) 10-12 or GD 12 caused hydrocephalus (Jordan et al., 1977; DeSesso and Goeringer, 1992). However, there are few reports to date

describing damage to the fetal brain following MTX administration to dams, and detailed effects of prenatal MTX treatment on fetal brain have been not completely elucidated even in experimental animals. Therefore, in the present study, we examined histopathologically the time-dependent changes of fetal brain following MTX administration to their dams on GD 13 to clarify pathogenesis of MTX-induced brain anomalies in fetuses.

2.2 Materials and methods

2.2.1 Animals

All experiments were performed using female Wistar Imamichi rats, 9 - 10 weeks of age, 218.45 ± 2.09 g (mean ± SE) in weight, and obtained from the Institute of Animal Reproduction (Kasumigaura, Japan). The animals were reared in a room with the temperature controlled at 22 ± 2°C, humidity at 50 ± 5%, with ventilation 11 times per hr, lighting at 12:12-hr light/dark cycle (light cycle, 7:00 - 19:00) and given standard chow (CE-2; Nihon Clea, Tokyo, Japan). The present experiments were performed following the provisions approved by the Animal Research Committee of Tottori University.

2.2.2 Experimental design

A total of 40 animals were divided into two groups as follows: (1) saline-treated control rats (*n*=20), (2) MTX-treated rats (*n*=20). MTX (Pfizer Japan Inc., Tokyo, Japan) was dissolved in saline. Day 0 of gestation (GD 0) was designated as the day when the presence of a vaginal plug was identified. The rats received intraperitoneal injections (i.p.) with MTX (30 mg/kg body weight) or saline (the control) on GD 13. The specific timing of MTX administration was selected, because the injection of DNA damaging chemicals, such as ethylnitrosourea (ENU) (Katayama et al., 2000; 2001; 2005), 6-mercaptopurine (6-MP) (Kanemitsu et al., 2009a), busulfan (Ohira et al., 2013), T-2 toxin (Sehata et al., 2004), 1-β-D-arabinofuranosylcytosine (Ara-C) (Yamauchi et al., 2004), 5-azacytidine (5AzC) (Ueno et al., 2002a; 2002b) and 5-Fluorouracil (5-Fu) (Yamaguchi et al., 2009) on GD13 induced apoptosis in neuroepithelial cells of telencephalon in rat fetal brain. The dose level in the present study was decided, because this dose was equivalent to 10% of the LD50 in intraperitoneal injection in rats (Johnson et al., 1994) or 15 % - 30 % of dosage used in high-dose cancer therapy in human (Hiraga et al., 1999; Komatsu et al., 1990). Fetus samples were collected under pentobarbital anesthesia (100 mg/kg, i.p.) 6, 12, 24, 36 and 48 hr, respectively, after MTX administration.

They were removed from the uterus and weighed, and their body lengths were measured.

2.2.3 Histopathological examination

For histopathological examination, all fetuses were fixed in 10% neutral buffered formalin and then embedded in paraffin. The tissues of telencephalon, diencephalon, mesencephalon and metencephalon in 12 fetal brain samples per group consisted of 3 fetuses ramdomly selected per dam in each group were sectioned at 2 μm thickness, stained with hematoxylin and eosin and examined with light microscopy. The number of pyknotic cells or mitotic cells was counted from over 1,000 neuroepithelial cells in the telencephalon, diencephalon, mesencephalon and metencephalon for each fetus by light microscopy, and the pyknotic index and mitotic index were calculated as the percentage of pyknotic cells or mitotic cells from out of the total number of neuroepithelial cells counted.

2.2.4 TUNEL method

DNA-fragmented neuroepithelial cells in telencephalon were detected by terminal deoxynucleotidyl-transferase (TdT)-mediated deoxyuridine

triphosphate-digoxigenin (dUTP) nick-end labeling (TUNEL), which was performed using an *in situ* apoptosis detection kit (Trevigen, Inc., Gaithersburg, MD, U.S.A.). The number of TUNEL-positive cells was obtained from over 1,000 neuroepithelial cells in the telencephalon for each fetus by light microscopy, and the TUNEL-index was calculated as the percentage of TUNEL-positive cells out of the total number of neuroepithelial cells counted.

2.2.5 Immunohistochemical examinations of rat fetuses

Immunohistochemical staining was performed by a labeled-polymer method using Histofine Simple Stain MAX-PO (R) (Nichirei, Tokyo, Japan). To retrieve the antigen, tissue sections for the detection of cleaved caspase-3 antigen were immersed in citrate buffer, pH 6.0 (Dako, Glostrup, Denmark) and autoclaved for 15 min at 121^{o}C; and tissue sections for the detection of phospho-histone H3 antigen were immersed in citrate buffer, pH 6.0 (Dako) and microwaved for 15 min. Endogenous peroxidase activity was quenched by immersing the sections in 3% hydrogen peroxide in methanol for 15 min. The sections were incubated with the cleaved caspase-3 rabbit polyclonal antibody (1:300 dilution; Cell Signaling Technology, Inc., Danvers, MA, U.S.A.) at 4^{o}C overnight; and the sections were incubated with the phospho-histone

H3 rabbit monoclonal antibody (1:1,500 dilution; Abcam, Tokyo, Japan) for 30 min at room temperature. Then, these sections were treated with Histofine Simple Stain MAX-PO (R) (Nichirei) for 30 min at room temperature. They were exposed to a 3,3′-diaminobenzidine solution containing hydrogen peroxide (Nichirei) to facilitate a peroxidase color reaction and then counterstained with Mayer's hematoxylin. The number of cleaved caspase-3- or phospho-histone H3-positive cells was counted from over 1,000 neuroepithelial cells in the telencephalon for each fetus by light microscopy, and the cleaved caspase-3- or phospho-histone H3-index was calculated as the percentage of cleaved caspase-3- or phospho-histone H3-positive cells out of the total number of neuroepithelial cells counted.

2.2.6 Statistical analysis

Means ± standard error (SE) of the individual litter value was calculated. The data were analyzed with an *F*-test. When variances were homogeneous, the Student's *t*-test was performed. Welch's *t*-test was employed when variances were not homogeneous ($P<0.05$). $P<0.05$, $P<0.01$ or $P<0.001$ was considered to be statistically significant.

2.3 Results

2.3.1 Effects of MTX on rat fetuses

Six, 12 and 24 hr after MTX treatment, there were no significant differences in the number of living fetuses per litter and the fetal mortality rates between the control group and MTX-treated group (Table 1). The number of living fetuses significantly declined, and fetal mortality rates significantly increased at 36 hr in the MTX-treated group, compared to those of the control group (Table 1). Almost all fetuses died by 48 hr after MTX treatment (Table 1).

2.3.2 Histopathological findings of rat fetal brain

In the control group, pyknotic changes in neuroepithelial cells were rarely observed in any layers of the telencephalic wall throughout the experimental period (Figs. 1 and 2).

Six hr after treatment in the MTX-treated group, pyknotic neuroepithelial cells appeared in the telencephalic wall and scattered throughout that wall (Fig. 1B). Then, 12 - 36 hr after MTX treatment, pyknotic neuroepithelial cells drastically increased and were diffusely distributed throughout the telencephalic wall (Figs. 1C - E and 2). At 36 hr, neuroepithelial cells were eliminated and showed low cell density in the

telencephalon of MTX-treated group (Fig. 1E). Although mitotic neuroepithelial cells were located along the ventricular layer of the telencephalic wall in the control group, they were rarely observed in the same region at 6 - 36 hr in the MTX-treated group (Fig. 1B - E).

In the telencephalon of the control group, TUNEL-positive neuroepithelial cells were rarely observed in any layers of the telencephalic wall throughout the experimental period (Figs. 3A and 4). Most of the pyknotic neuroepithelial cells were positively stained by the TUNEL method at 12, 24 and 36 hr in the MTX-treated group (Fig. 3C - E), while there were few pyknotic neuroepithelial cells positively stained by the TUNEL method at 6 hr (Fig. 3B). In the MTX-treated group, the index of TUNEL-positive neuroepithelial cells in the telencephalic wall significantly increased at 12 and 24 hr and peaked at 36 hr (Fig. 4).

Cleaved caspase-3-positive neuroepithelial cells were rarely observed in the telencephalon of control group throughout the experimental period (Figs. 5A and 6), although in the MTX-treated group, almost all pyknotic neuroepithelial cells were immunohistochemically positive for cleaved caspase-3 throughout the experimental period (Fig. 5B - E). In the MTX-treated group, the index of cleaved caspase-3-positive neuroepithelial cells in the telencephalon significantly increased at

6, 12 and 24 hr and peaked at 36 hr (Fig. 6).

Phospho-histone H3-positive neuroepithelial cells were located along the ventricular layer of the telencephalic wall in the control group, while there were fewer phospho-histone H3-positive cells at 6 - 36 hr in the same region of the MTX-treated group than in the control group (Fig. 7A - E). The index of phospho-histone H3-positive neuroepithelial cells in telencephalon decreased significantly at 6 hr compared with the control group and maintained that low level throughout the experimental period (Fig. 8).

In the MTX-treated group, pyknotic indices of telencephalon and diencephalon significantly increased at 12 - 36 hr, and those of the mesencephalon significantly increased at 24 and 36 hr, compared to the control group (Table 2). The pyknotic index of metencephalon significantly increased at 36 hr compared to control group, and it showed a clearly lower value, compared to those of the telencephalon, diencephalon and mesencephalon (Table 2). In the MTX-treated group, there were fewer pyknotic neuroepithelial cells in the metencephalon than in the telencephalon, diencephalon and mesencephalon. In the MTX-treated group, while mitotic indices of telencephalon, diencephalon and mesencephalon decreased significantly at 6 - 36 hr, that of metencephalon decreased significantly at 6 and 12 hr compared to the control

group (Table 3).

2.4 Discussion

It has been reported that microcephaly can occur as one of the central nervous system anomalies of MTX embryopathy in humans (Bawle et al., 1998; Garcia-Minaur and Botella, 2000). The pathogenesis of microcephaly was closely associated with excessive neuronal death (Furukawa et al., 2004; Takano et al., 2006; Passemard et al., 2013). The cause of MTX-induced microcephaly may be also associated with excessive neuronal death. In the present study, the majority of pyknotic neuroepithelial cells in the telencephalic wall were positive for TUNEL staining and cleaved caspase-3. Cleavage of caspase-3 is known to be involved in cell apoptosis, and is recognized as an apoptosis marker (Gown and Willingham, 2002). These results indicate that pyknotic changes induced by MTX in the present study are caused by apoptosis. In the present study, pyknotic neuroepithelial cells in the telencephalon at 6 hr were positive for cleaved caspase-3, but negative for TUNEL staining. This result may reflect that the cleavage of caspase-3 precedes DNA fragmentation in the process of the neuroepithelial cell apoptosis induced by MTX.

The previous studies showed that DNA-damaging chemical administration at

GD 12 or 13 induces apoptosis in neuroepithelial cells of the telencephalic wall of fetal brain (Katayama et al., 2000; 2001; Ueno et al., 2002a; 2002b; Woo et al., 2003; Katayama et al., 2005; Nam et al., 2006; Yamaguchi et al., 2009; Ohira et al., 2013). These apoptotic neuroepithelial cells are mainly observed in the dorsal layer after treatment with ENU (Katayama et al., 2000; 2001; 2005; Doi, 2011) in the medial to dorsal layer after treatment with hydroxyurea (Woo et al., 2003), 5-Fu (Yamaguchi et al., 2009; Doi, 2011), busulfan (Ohira et al., 2013) and etoposide (Nam et al., 2006) and in the ventral to medial layers after treatment with 5AzC (Ueno et al., 2002a; 2002b; Doi, 2011). In the present study, apoptotic neuroepithelial cells localized throughout all layers of the telencephalic wall, but their distribution was different from those of apoptotic neuroepithelial cells induced by the above-mentioned other DNA-damaging chemicals (Table 4). It is known that in the ventricular zone of fetal brain, the positions of the nuclei of neuroepithelial cells are correlated with their cell cycle phase (Doi, 2011). S-phase nuclei are located in the dorsal layer of the ventricular zone (Doi, 2011). They migrate inward during the G2 phase, and mitosis occurs at the ventricular surface (Doi, 2011). Then, they migrate outward during the G1 phase and enter the S phase again (Doi, 2011). In brief, the nuclei during the G1 or G2 phase are in the middle layer of the ventricular zone. The distribution of apoptotic

neuroepithelial cells throughout all layers of the telencephalic wall in the present study may reflect that MTX induces apoptosis of neuroepithelial cells in all phases of the cell cycle or that apoptosis occurs independently of cell cycle arrest. Whereas a previous study showed that apoptosis of the human hepatoma HepG2 cells induced by folate deficiency was specific for S- and/or G2-phase arrest (Huang et al., 1999), the present result suggests that MTX induces apoptosis of neuroepithelial cells through a mechanism other than S- and/or G2-phase arrest.

In the present study, the pyknotic, TUNEL and cleaved caspase-3 indices of neuroepithelial cells in the telencephalon peaked 36 hr after treatment with MTX at GD 13 (Table 5). The index of pyknotic cells in the telencephalon peaked 9 - 12 hr after treatment with Ara-C (Yamauchi et al., 2004) and ENU (Katayama et al., 2001). The index of TUNEL-positive cells peaked 12 hr after treatment with T-2 toxin (Sehata et al., 2004) and 5AzC (Ueno et al., 2002a), and the index of cleaved caspse-3-positive cells peaked 48 hr after treatment with busulfan (Ohira et al., 2013). On the other hand, in the present study, mitotic and phospho-histone H3 indices in telencephalon treated with MTX decreased significantly at 6 hr and maintained that low level throughout the experimental period (Table 5). The mitotic cell index in the telencephalon significantly decreased at 30 hr and reached its lowest level 36 hr after

treatment with 6-MP (Kanemitsu et al., 2009a), while the mitotic cell index peaked 6 hr, decreased thereafter and reached the minimal level 24 hr after treatment with 5AzC (Ueno et al., 2002b). The index of phospho-histone H3-positive cells significantly decreased at 24 hr and reached its minimal level 48 hr after treatment with busulfan (Ohira et al., 2013), while it reached the lowest level 36 hr after treatment with 6-MP (Kanemitsu et al., 2009b). The distribution of pyknotic neuroepithelial cells and the time-course changes of the indices of pyknotic and mitotic neuroepithelial cells in the telencephalic wall were different from those of the previously-mentioned other DNA-damaging chemicals. These differences may reflect the disparity in mechanisms of apoptosis and the inhibition of cell proliferation in neuroepithelial cells among DNA-damaging chemicals. Further investigations should be conducted to clarify the true cause of these differences.

In the present study, MTX induced fewer pyknotic changes of neuroepithelial cells in the metencephalon than in other brain regions. The result of a previous study suggested that cell-proliferative activity was associated with the sensitivity to MTX (Sun et al., 2013). The different pyknotic indices of the MTX-treated group among the brain regions in the present study may reflect the disparity of cell-proliferative activity. In a previous study (Zamenhof, 1985), MTX inhibited the development of individual

brain parts to varying degrees in chick embryos. The same study suggested that the different effects of MTX on various brain parts may be due to different schedules of cell proliferation among individual brain parts. Other previous studies demonstrated that busulfan or 5-Fu treatment at GD13 in rat fetus induced pyknotic changes of neuroepithelial cells in metencephalon to the same degree as those in diencephalon and mesencephalon (Ohira et al., 2009; Yamaguchi et al., 2009). These results suggest that there are differences in sensitivities to MTX, busulfan and 5-Fu of neuroepithelial cells in the metencephalon.

There are several studies describing brain malformation induced by MTX in human and rabbits (Jordan et al., 1977; Seidahmed et al., 2006; Corona-Rivera et al., 2010). A report of Seidahmed *et al.* (2006) described that 2.5 mg of MTX 3 times a day for 7 days, for a total of 52.5 mg at 6 weeks of gestation, induced alobar holoprosencephaly, cerebellar hypoplasia and agenesis of the corpus callosum in human. Corona-Rivera *et al.* (2010) reported that MTX 5mg/day treatment for 14 days at the 5th week post-conception induced brain anomalies including semilobar holoprosencephaly and hydrocephalus in human. In rabbits, MTX 19.2 mg/kg administration during GD 10-15 induced various anomalies including hydrocephalus (Jordan et al., 1977). In the present study, single dose-administration of MTX 30

mg/kg on GD 13 induced fetal death 48 hr after treatment, and the cause of fetal death in the present study may be relevant to dose, number and timing of MTX administration.

In conclusion, MTX administration of 30 mg/kg on GD 13 induced apoptosis of neuroepithial cells and inhibited mitosis of these cells in telencephalon 6 - 36 hr after treatment. The distribution of apoptotic neuroepithelial cells in the telencephalic wall and the whole brain and the time-course changes of the indices of apoptotic and mitotic neuroepithelial cells were different from other DNA-damaging chemicals reported previously. While the detailed mechanisms of MTX-induced neuroepithelial cell damage in fetal brain remain unclear, the present results provide fundamental information about the fetal brain damage induced by MTX. The present results serve to elucidate the pathogenesis of nervous system anomalies resulting from failed pregnancy termination with MTX or when mothers who are taking MTX for medical reasons become pregnant inadvertently. To our knowledge, this is the first report demonstrating histopathological findings of fetal brain damage induced by MTX.

Table 1. Effects of methotrexate on rat fetuses

	Treatment	No. of dams	Total No. of live fetuses	Living fetuses per litter	Dead fetus ratio (%)
6 hr	Control	4	58	14.59 ± 0.50	9.03 ± 3.03
	MTX	4	57	14.25 ± 0.63	3.14 ± 1.82
12 hr	Control	4	56	14.00 ± 0.41	7.93 ± 3.00
	MTX	4	63	15.75 ± 2.50	15.92 ± 10.67
24 hr	Control	4	58	14.50 ± 1.44	7.63 ± 4.81
	MTX	4	57	14.25 ± 0.95	6.48 ± 4.44
36 hr	Control	4	62	15.50 ± 1.19	3.58 ± 3.58
	MTX	4	44	11.00 ± 0.41*	30.30 ± 5.41**
48 hr	Control	4	56	14.00 ± 1.00	4.73 ± 3.15
	MTX	4	1	0.25 ± 0.25†††	98.53 ± 1.48***

Values are expressed as means ± SE.

*, **, ***: Significantly different from control at P<0.05, P<0.01, P<0.001, respectively (Student's *t*-test).

†††: Significantly different from control at P<0.001 (Welch's *t*-test).

Table 2. Pyknotic index (%) in rat fetal brain treated by MTX

		6 hr	12 hr	24 hr	36 hr
Telencephalon	Control	0.03 ± 0.03	0.05 ± 0.05	0.10 ± 0.07	0.28 ± 0.14
	MTX	2.68 ± 0.85	19.98 ± 2.45††	34.82 ± 2.17†††	43.33 ± 3.07†††
Diencephalon	Control	0.61 ± 0.28	0.79 ± 0.30	0.66 ± 0.36	0.81 ± 0.30
	MTX	1.61 ± 0.38	14.31 ± 1.53††	20.88 ± 2.44††	20.65 ± 1.67††
Mesencephalon	Control	0.39 ± 0.04	0.41 ± 0.11	0.29 ± 0.11	0.47 ± 0.12
	MTX	0.37 ± 0.18	7.78 ± 2.88	26.90 ± 5.45†	36.56 ± 3.99††
Metencephalon	Control	0.00 ± 0.00	0.00 ± 0.00	0.00 ± 0.00	0.07 ± 0.05
	MTX	0.04 ± 0.02	0.00 ± 0.00	2.34 ± 1.52	3.88 ± 0.72†

Values are expressed as means ± SE (%).

†, ††, †††: Significantly different from control at $P<0.05$, $P<0.01$, $P<0.001$ respectively (Welch's *t*-test).

Table 3. Mitotic index (%) in rat fetal brain treated by MTX

		6 hr	12 hr	24 hr	36 hr
Telencephalon	Control	4.56 ± 0.20	4.48 ± 0.25	4.82 ± 0.24	4.50 ± 0.09
	MTX	0.53 ± 0.05†††	0.24 ± 0.03†††	0.16 ± 0.08***	0.22 ± 0.13***
Diencephalon	Control	3.01 ± 0.28	3.30 ± 0.33	2.56 ± 0.36	3.66 ± 0.28
	MTX	0.37 ± 0.08***	0.57 ± 0.09***	0.37 ± 0.09††	0.40 ± 0.20***
Mesencephalon	Control	3.64 ± 0.43	3.76 ± 0.35	3.51 ± 0.44	4.53 ± 0.34
	MTX	0.64 ± 0.17***	0.96 ± 0.10***	0.22 ± 0.07††	1.13 ± 0.27***
Metencephalon	Control	3.12 ± 0.64	3.25 ± 0.25	1.37 ± 0.25	1.25 ± 0.10
	MTX	0.67 ± 0.08†	1.40 ± 0.35**	1.53 ± 0.47	1.60 ± 0.26

Values are expressed as means ± SE (%).

, *: Significantly different from control at P<0.01, P<0.001 respectively (Student's *t*-test).

†, ††, †††: Significantly different from control at P<0.05, P<0.01, P<0.001 respectively (Welch's *t*-test).

Table 4. Location of apoptotic cells in the ventricular zone of telencephalon after treatment with DNA-damaging chemicals

	Location of apoptotic cells in the ventricular zone of telencephalon
Ethylnitrosourea	Dorsal layer
Hydroxyurea, Busulfan, Etoposide, 5-Fluorouracil	Medial to dorsal layers
5-Azacytidine	Ventral to medial layers
Methotrexate	All layers

Table 5. Timing of the maximal level of cell death indices and minimal level of cell proliferation indices in the telencephalon after DNA-damaging chemicals treatment

	Maximal level of cell death indices			Minimal level of cell proliferation indices	
	Pyknosis	TUNEL	Cleaved caspase-3	Mitosis	Phospho-histone H3
1-β-D-arabinofuranosylcytosine	9 hr	—	—	—	—
Ethylnitrosourea	12 hr	—	—	—	—
T-2 toxin	—	12 hr	—	—	—
5-azacytide	—	12 hr	—	24 hr	—
Busulfan	—	—	48 hr	—	48 hr
6-Mercaptopurine	—	—	—	36 hr	36 hr
Methotrexate	36 hr	36 hr	36 hr	6 - 36 hr	6 - 36 hr

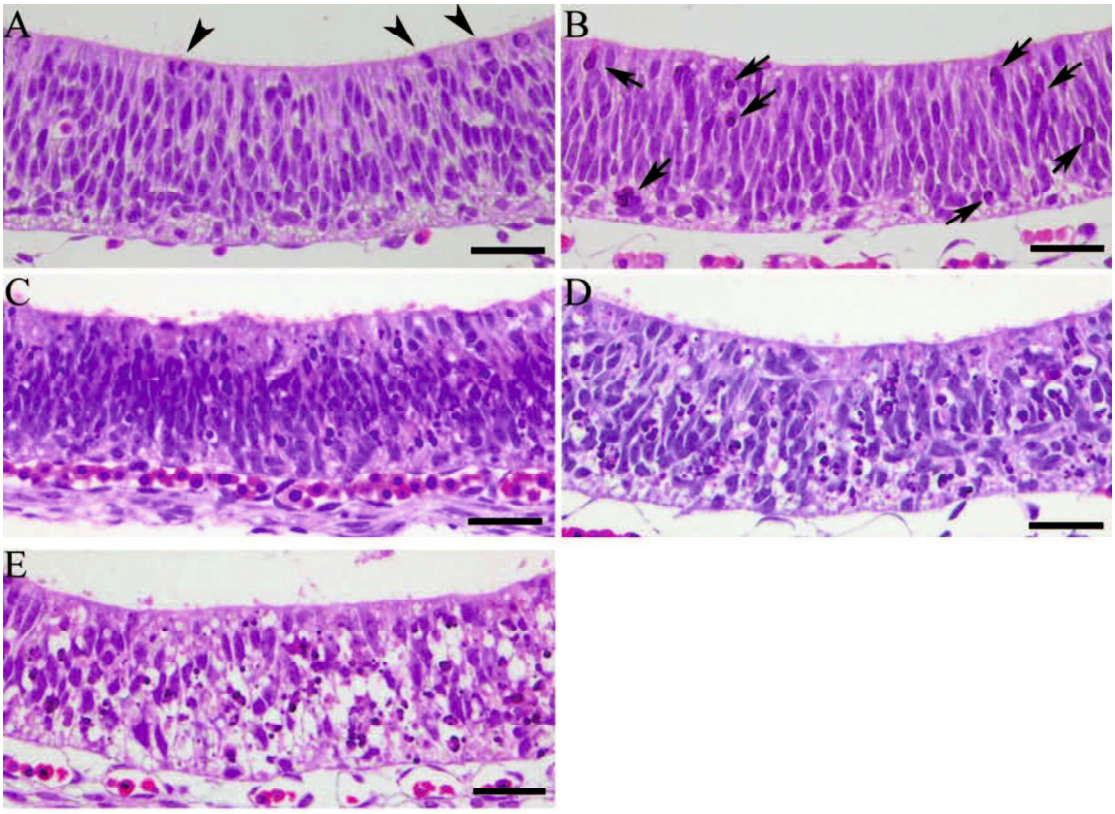

Fig. 1. Histopathological findings of telencephalic wall of rat fetal brain in the control group 6 hr after treatment (A) and the MTX-treated group at 6 (B), 12 (C), 24 (D) and 36 hr (E), respectively. (A) Arrowheads indicate mitotic cells. (B) Arrows indicate pyknotic cells. Bar=30 μm.

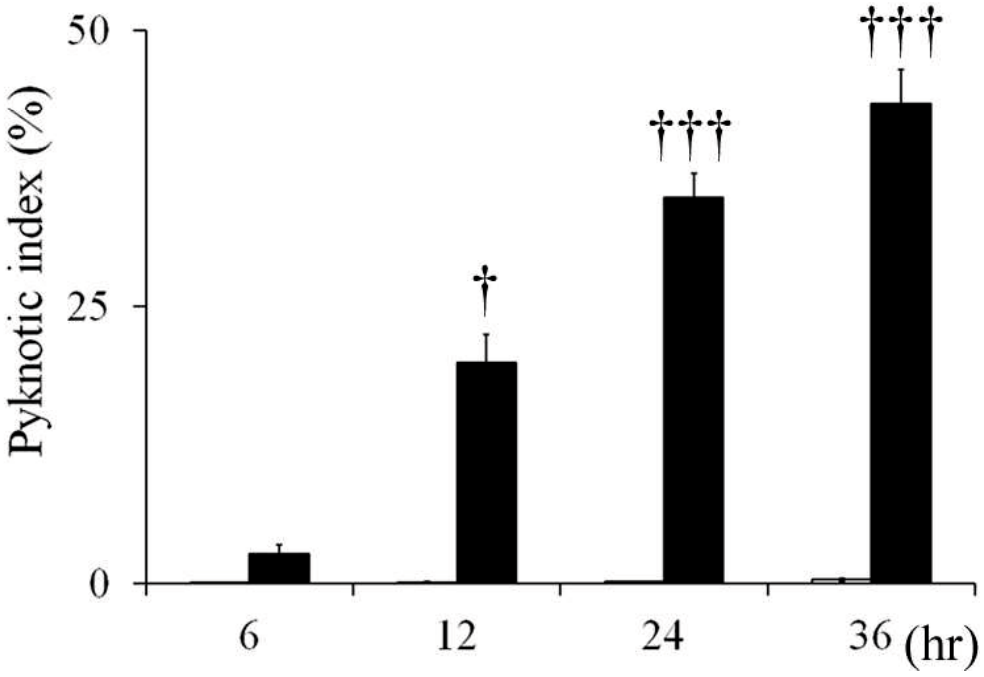

Fig. 2. Changes in the pyknotic index (%) in telencephalic wall of rat fetal brain. Values are expressed as means ± SE. †, †††: Significantly different from control at $P<0.05$, $P<0.001$, respectively (Welch's *t*-test).

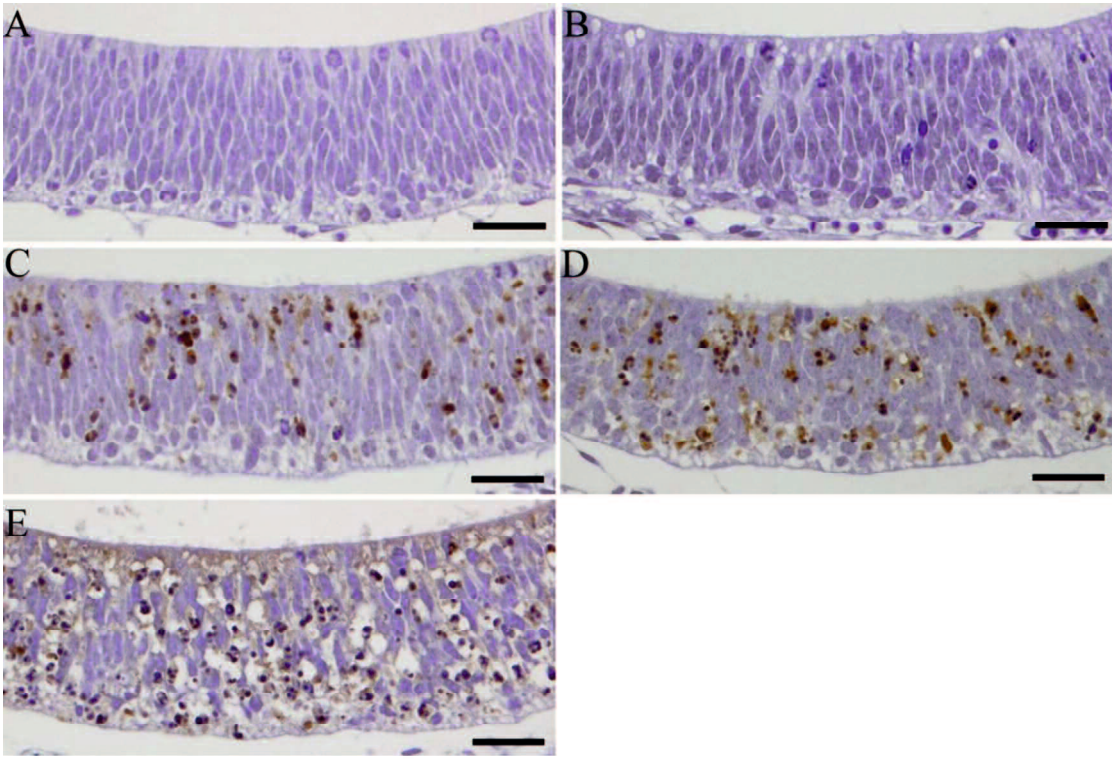

Fig. 3. TUNEL-positive cells in telencephalic wall of rat fetal brain in the control group 6 hr after treatment (A) and the MTX-treated group at 6 (B), 12 (C), 24 (D) and 36 hr (E). Bar=30 μm.

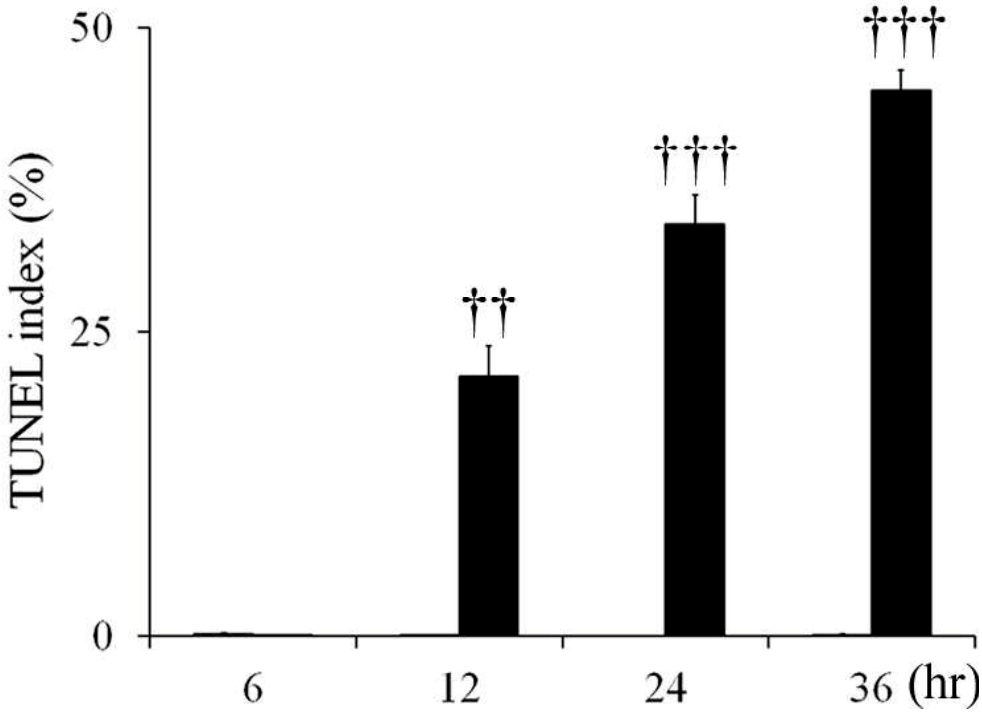

Fig. 4. Changes in the TUNEL index (%) in telencephalic wall of rat fetal brain. Values are expressed as means ± SE. ††, †††: Significantly different from control at P<0.01, P<0.001, respectively (Welch's *t*-test).

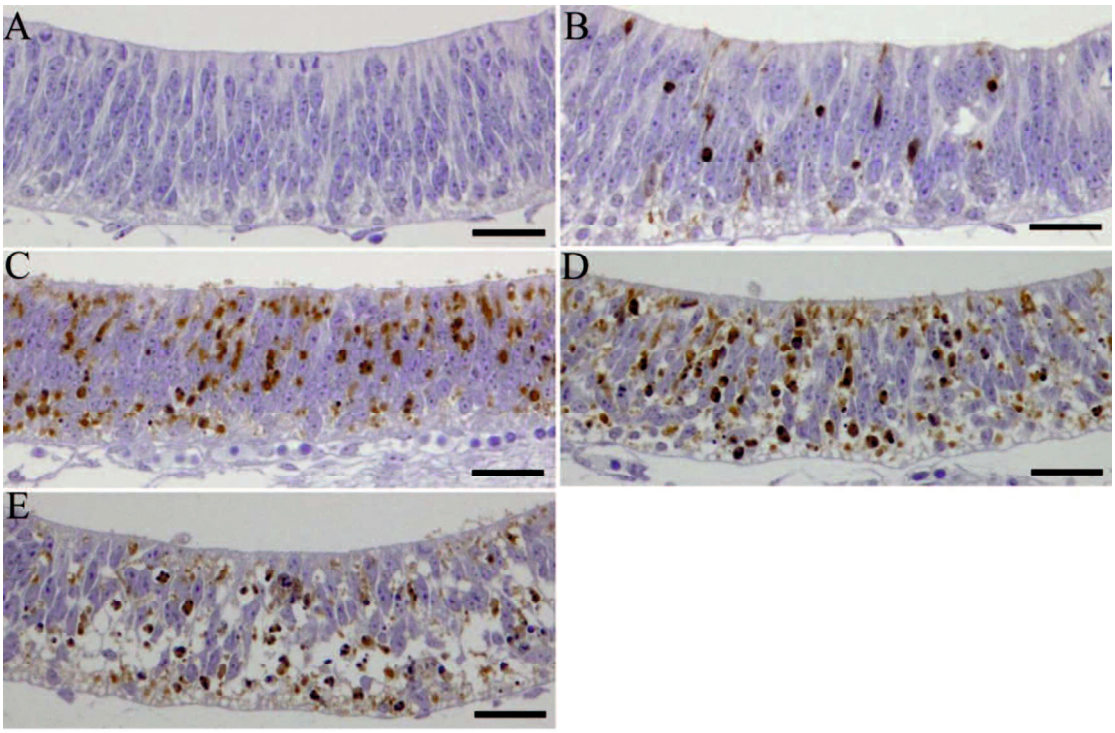

Fig. 5. Immunohistochemical expression of cleaved caspase-3 in telencephalic wall of rat fetal brain in the control group 6 hr after treatment (A) and the MTX-treated group at 6 (B), 12 (C), 24 (D) and 36 hr (E). Bar=30 μm

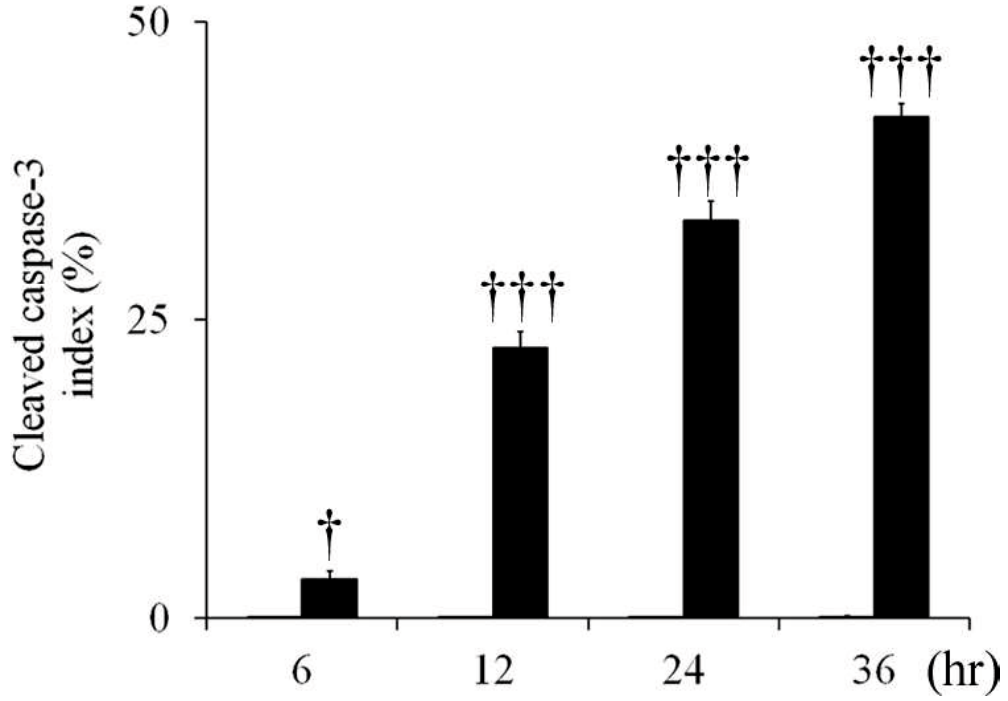

Fig. 6. Cleaved caspase-3 index. Values are expressed as means ± SE. †, †††: Significantly different from control at $P<0.05$, $P<0.001$, respectively (Welch's *t*-test).

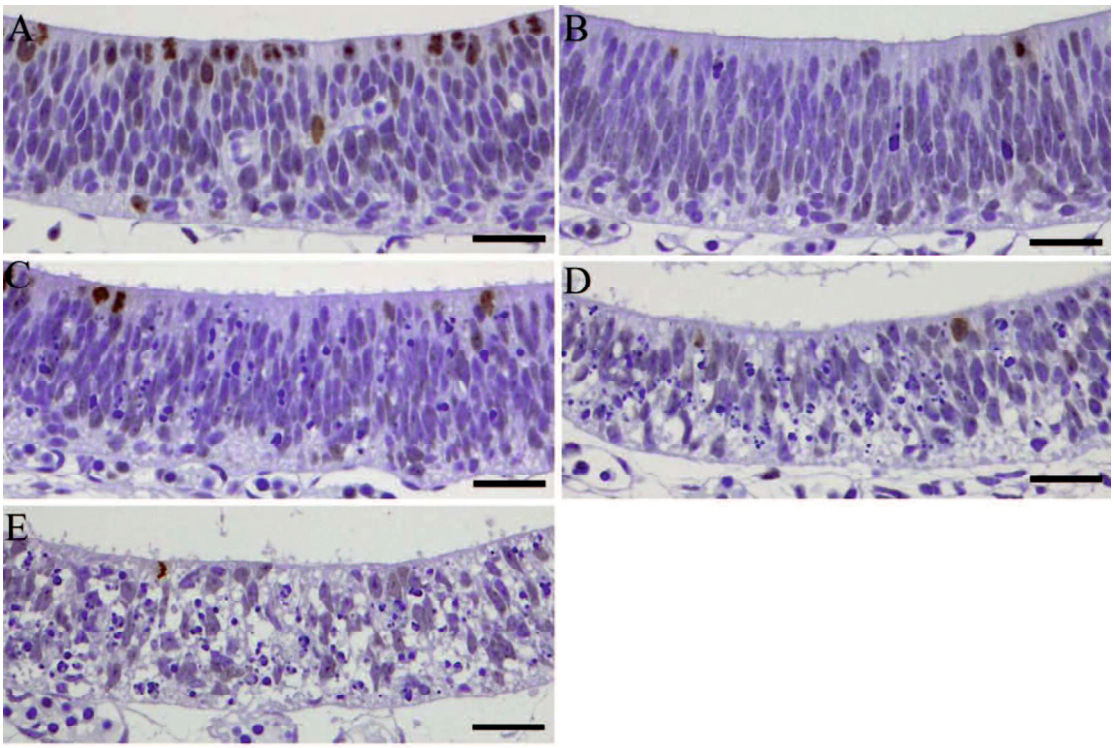

Fig. 7. Immunohistochemical expression of phospho-histone H3 in telencephalic wall of in rat fetal brain in the control group 6 hr after treatment (A) and the MTX-treated group at 6 (B), 12 (C), 24 (D) and 36 hr (E), respectively. Bar=30 μm.

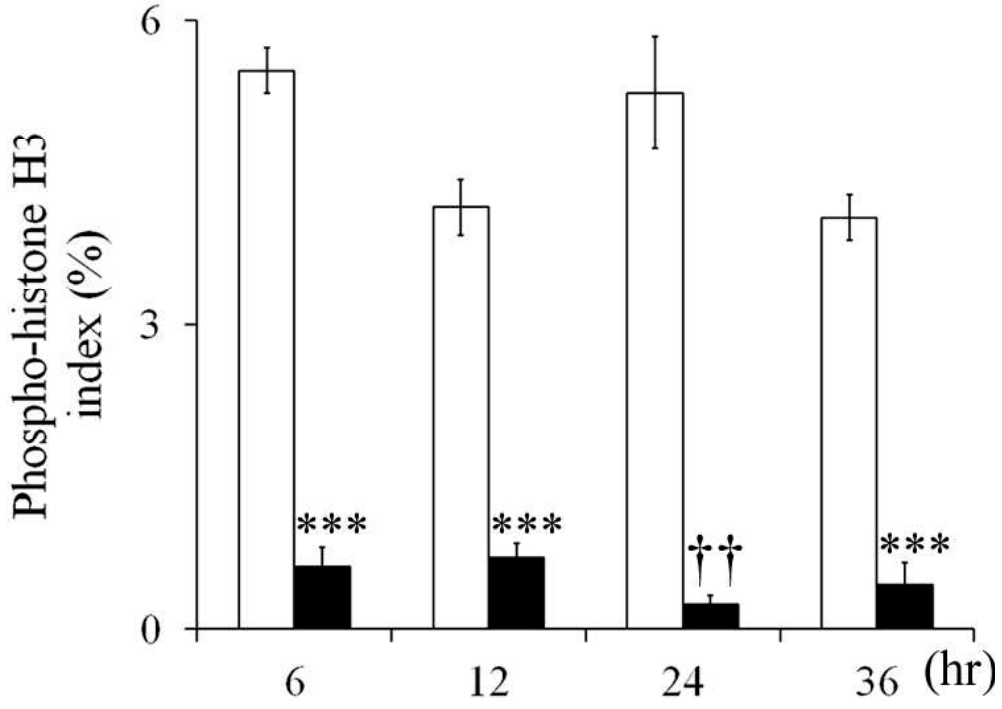

Fig. 8. Phospho-histone H3 index. Values are expressed as means ± SE. ***: Significantly different from control at P<0.001 (Student's *t*-test). ††: Significantly different from control at P<0.01 (Welch's *t*-test).

GENERAL CONCLUSION

In the first chapter, we aimed to obtain clues to clarify the role of the placenta in the induction of MTX-induced fetal developmental disability. MTX treatment at 0.2 mg/kg/day during GDs 13-14 induced few pathological changes in the placenta, whereas MTX administration during GDs 11-12 induced growth arrest of basal and labyrinth zones, leading to small placentas, in addition to the increase of fetal mortality rates and the decrease of fetal weights. Particularly, the hypoplasia of the basal zone induced by MTX exposure during GDs 11-12 was more severe than that of the labyrinth zone. Moreover, a significant increase in apoptotic cells and a significant decrease in mitotic cells were detected in the basal zone of GD11- and 12-treated group. These results suggested that the component cells of the basal and labyrinth zones on GDs 11-12 are more highly sensitive to MTX than those during GDs 13-14 and that MTX affects the component cells of the basal zone more strongly than those of the labyrinth zone. While it is speculated that basal zone hypoplasia correlates with the fetal mortality rate and decrease of fetal weights, the fact remains unclear. To our knowledge, this is the first published report demonstrating the sequential histopathological findings of placental growth retardation induced by MTX.

In the second chapter, the study aimed to clarify the pathogenesis of

MTX-induced brain anomalies in fetuses. MTX administration of 30 mg/kg on GD 13 induced apoptosis of neuroepithial cells and inhibited proliferative activity of these cells in the ventricular zone of telencephalon. The time-course changes of the indices of apoptosis and cell proliferation were different from other DNA-damaging chemicals reported previously. These differences may reflect the disparity in pharmacokinetics and mechanisms of DNA damage, apoptosis and the inhibition of cell proliferation in neuroepithelial cells among DNA-damaging chemicals. In addition, the distribution of apoptotic neuroepithelial cells throughout all layers of the telencephalon in the present study, and it is different from other DNA-damaging chemicals. It is speculated that MTX induces apoptosis of neuroepithelial cells in all phases of the cell cycle or that apoptosis occurs independently of cell cycle arrest. The present results provide fundamental information about the MTX-induced fetal brain damage and contribute to elucidate the pathogenesis of brain anomalies in MTX embryopathy. To our knowledge, this is the first study demonstrating the time-dependent histopathological findings of fetal brain damage induced by MTX, although the exact mechanisms of MTX-induced neuroepithelial cell damage in fetal brain need to be clarified by further study.

ABSTRACT

In chapter 1, the sequential changes in the placenta from rats exposed to MTX were examined histopathologically. MTX was intraperitoneally administered at 0.2 mg/kg/day during gestation days (GDs) 11-12 or GDs 13-14, and the placentas were sampled on GDs 13, 15, 17 and 21. The fetal mortality rates tended to increase throughout the experimental period, and fetal weights were significantly decreased on GD13 in the GD11,12-treated group. A significant reduction in placental weights was detected on GDs 13 and 15 in the GD11,12-treated group. Histopathologically, in the GD11,12-treated group, a significant thinning of the basal zone was detected throughout the experimental period, whereas the thickness of the labyrinth zone decreased significantly during GDs 13-17. The severity of thinning of the basal zone was higher than that of the labyrinth zone. In addition, a marked decrease in glycogen cell-islands in the basal zone was detected on GD 15. A significant decrease in Phospho-Histone H3-positive cells and a significant increase in TUNEL-positive cells were detected on GD 13 in the basal zone of the GD11,12-treated group. In the GD13,14-treated group, there were no other significant changes in placentas and fetuses throughout the experimental period other than thinning of the labyrinth zone on GD 17. These results suggest that component cells of the basal and labyrinth zones

during GDs 11-12 are more highly sensitive for MTX than those during GDs 13-14 and MTX affects the component cells of basal zone more strongly than those of the labyrinth zone.

In chapter 2, the study was aimed to elucidate the pathogenesis of the damage of fetal brain induced by MTX. Pregnant rats were treated with 30 mg/kg of MTX on gestation day 13, and fetal brains were examined histopathologically from 6 to 48 hr after the treatment. In the telencephalon of the control group, there were few pyknotic neuroepithelial cells throughout the experimental period. Six hr after MTX treatment, several pyknotic neuroepithelial cells scattered throughout the telencephalic wall. At 12 - 36 hr, pyknotic neuroepithelial cells increased significantly and were diffusely distributed throughout the telencephalic wall. Neuroepithelial cells were eliminated and showed sparse cell density at 36 hr in the telencephalon. Almost all fetuses died at 48 hr. Most of the pyknotic neuroepithelial cells were positively stained by the TUNEL method and positive for cleaved caspase-3. While mitotic and phospho-histone H3-positive neuroepithelial cells were located along the ventricular layer of telencephalon in the control group, they were rarely observed in the same region at 6 - 36 hr in the MTX-treated group. MTX induced few pyknotic changes to neuroepithelial cells in the metencephalon, compared to other parts of brain. The

distribution of apoptotic neuroepithelial cells and the time-course changes of the indices of apoptotic and mitotic neuroepithelial cells were different from those of other DNA-damaging chemicals reported previously. The difference may reflect the disparity in mechanisms of apoptosis and the inhibition of cell proliferation in neuroepithelial cells induced by MTX.

ACKNOWLEDGEMENTS

The research for this PhD-thesis was carried out at the Department of Veterinary Laboratory Medicine, Faculty of Agriculture, Tottori University, Japan. I would like to express my sincere appreciation and gratitude to my principal supervisor Associate Professor Dr. Akihiko Sugiyama (Tottori University), for his firm guidance and encouragement during this study. It is indeed my great honor to have learned a lot under his supervising. His broad theoretical knowledge in the veterinary medicine, his precise academic manner has deeply touched me.

I am deeply grateful to Professor Dr. Takashi Takeuchi (Tottori University) for giving me the opportunity to study in this well developed laboratory and I would like to thank him for the firm guidance and kind support. And great thanks to Professor Dr. Masaru Okuda (Yamaguchi University) for his expert advice and for sharing his amazing scientific insight. I also want to thank Professor Dr. Yoshiaki Hikasa and Professor Dr. Takehito Morita for critical review of this thesis.

Also I wish to thank all members of the Department of Veterinary Laboratory Medicine (Tottori University), particularly to Mr. Shota Inoue, Mr. Kota Ueda, Ms. Ayano Hirako and Ms. Kana Shimohashi, for their great helping during this study.

I would like to express my thanks to the officers of United Graduate School of

Veterinary Science (Yamaguchi University) and Center for International Affairs (Tottori University) for the kind support during my life.

I would like to thank Japanese government and JGC-S scholarship foundation for the financial support.

Finally, I want to express my heartfelt gratitude to my family for their support and warm encouragement all the time.

REFERENCES

Acar N, Korgun ET, Cayli S, Sahin Z, Demir R, Ustunel I. Is there a relationship between PCNA expression and diabetic placental development during pregnancy? Acta Histochemica 2008;110:408-17.

Adamson SL, Lu Y, Whiteley KJ, Holmyard D, Hemberqer M, Pfarrer C, et al. Interactions between trophoblast cells and the maternal and fetal circulation in the mouse placenta. Developmental Biology 2002;250:358-73.

Ain R, Canham LN, Soares MJ. Gestation stage-dependent intrauterine trophoblast cell invasion in the rat and mouse: novel endocrine phenotype and regulation. Developmental Biology 2003;260:176-90.

Bauer MK, Harding JE, Bassett NS, Breier BH, Oliver MH, Gallaher BH, et al. Fetal growth and placental function. Molecular and Cellular Endocrinology 1998;140:115-20.

Bawle EV, Conard JV, Weiss L. Adult and two children with fetal methotrexate syndrome. Teratology 1998;57:51-5.

Bouillot S, Rampon C, Tillet E, Huber P. Tracing the glycogen cells with protocadherin 12 during mouse placenta development. Placenta 2006;27:882-8.

Ciaccio M, Bivona G, Bellia C. Therapeutical approach to plasma homocysteine and

cardiovascular risk reduction. Therapeutics and Clinical Risk Management 2008;4:219-24.

Coan PM, Conroy N, Burton GJ, Ferguson-Smith AC. Origin and characteristics of glycogen cells in the developing murine placenta. Developmental Dynamics 2006;235:3280-94.

Corona-Rivera JR, Rea-Rosas A, Santana-Ramírez A, Acosta-León J, Hernández-Rocha J, Miguel-Jiménez K. Holoprosencephaly and genitourinary anomalies in fetal methotrexate syndrome. American Journal of Medical Genetics. Part A 2010;152:1741-6.

Creinin MD, Krohn M. Methotrexate pharmacokinetics and effects in women receiving methotrexate 50 mg and 60 mg per square meter for early abortion. American Journal of Obstetrics and Gynecology 1997;177:1444-9.

Cronstein BN. Low-dose methotrexate: a mainstay in the treatment of rheumatoid arthritis. Pharmacological Reviews 2005;57:163-72.

Cuellar ML, Espinoza LR. Methotrexate use in psoriasis and psoriatic arthritis. Rheumatic Diseases Clinics of North America 1997;23:797-809.

Davies J, Glasser SR. Histological and fine structural observations on the placenta of the rat. Acta Anatomica (Basel) 1968;69:542-608.

Del Campo M, Kosaki K, Bennett FC, Jones KL. Developmental delay in fetal aminopterin/methotrexate syndrome. Teratology 1999;60:10-2.

DeLoia JA, Stewart-Akers AM, Creinin MD. Effects of methotrexate on trophoblast proliferation and local immune responses. Human Reproduction 1998;13:1063-9.

DeSesso JM, Goeringer GC. Methotrexate-induced developmental toxicity in rabbits is ameliorated by 1-(p-tosyl)-3,4,4-trimethylimidazolidine, a functional analog for tetrahydrofolate-mediated one-carbon transfer. Teratology 1992;45:271-83.

Doi K. Mechanisms of neurotoxicity induced in the developing brain of mice and rats by DNA-damaging chemicals. The Journal of Toxicological Sciences 2011;36:695-712.

Furukawa S, Abe M, Usuda K, Ogawa I. Indole-3-acetic acid induces microencephaly in rat fetuses. Toxicologic Pathology 2004;32:659-67.

Furukawa S, Hayashi S, Usuda K, Abe M, Hagio S, Ogawa I. Toxicological pathology in the rat placenta. Journal of Toxicologic Pathology 2011;24:95-111.

Furukawa S, Hayashi S, Usuda K, Abe M, Hagio S, Ogawa I. Effect of cisplatin on rat placenta development. Experimental and Toxicologic Pathology 2013;65:211-7.

Furukawa S, Usuda K, Abe M, Hayashi S, Ogawa I. Effect of 6-mercaptopurine on rat placenta. Journal of Veterinary Medical Science 2008;70:551-6.

Garcia-Minaur S, Botella MP. Further case of aminopterin syndrome sine aminopterin in a Spanish child. American Journal of Medical Genetics 2000;95:320-4.

Genestier L, Paillot R, Quemeneur L, Izeradjene K, Revillard JP. Mechanisms of action of methotrexate. Immunopharmacology 2000;47:247-57.

Gown AM, Willingham MC. Improved detection of apoptotic cells in archival paraffin sections: immunohistochemistry using antibodies to cleaved caspase 3. The Journal of Histochemistry and Cytochemistry 2002;50:449-54.

Griffith TM, Chaytor AT, Bakker LM, Edwards DH. 5-Methyltetrahydrofolate and tetrahydrobiopterin can modulate electrotonically mediated endotheliumdependent vascular relaxation. Proceedings of the National Academy of Sciences of the United States of America 2005;102:7008-13.

He Y, Smith SK, Day KA, Clark DE, Licence DR, Charnock-Jones DS. Alternative splicing of vascular endothelial growth factor (VEGF)-R1 (FLT-1) pre-mRNA is important for the regulation of VEGF activity. Molecular Endocrinology 1999;13:537-45.

Herman S, Zurgil N, Deutsch M. Low dose methotrexate induces apoptosis with reactive oxygen species involvement in T lymphocytic cell lines to a greater extent than in monocytic lines. Inflammation Research 2005;54:273-80.

Hiraga S, Arita N, Ohnishi T, Kohmura E, Yamamoto K, Oku Y, et al. Rapid infusion of high-dose methotrexate resulting in enhanced penetration into cerebrospinal fluid and intensified tumor response in primary central nervous system lymphomas. Journal of Neurosurgery 1999;91:221-30.

Huang RF, Ho YH, Lin HL, Wei JS, Liu TZ. Folate deficiency induces a cell cycle-specific apoptosis in HepG2 cells. The Journal of Nutrition 1999;129:25-31.

Hyoun SC, Običan SG, Scialli AR. Teratogen update: methotrexate. Birth Defects Research. Part A, Clinical and Molecular Teratology 2012;94:187-207.

Ishihara N, Matsuo H, Murakoshi H, Laoap-Fernandez J, Samoto T, Maruo T. Changes in proliferative potential, apoptosis and Bcl-2 protein expression in cytotrophoblasts and syncytiotrophoblast in human placenta over the course of pregnancy. Endocrine Journal 2000;47:317-27.

Johnson FE, Farr SA, Mawad M, Woo YC. Testicular cytotoxicity of intravenous methotrexate in rats. Journal of Surgical Oncology 1994;55:175-8.

Jolivet J, Cowan KH, Curt GA, Clendeninn NJ, Chabner BA. The pharmacology and clinical use of methotrexate. New England Journal of Medicine 1983;309:1094-104.

Jordan RL, Wilson JG, Schumacher HJ. Embryotoxicity of the folate antagonist methotrexate in rats and rabbits. Teratology 1977;15:73-9.

Joshi R, Adhikari S, Patro BS, Chattopadhyay S, Mukherjee T. Free radical scavenging behavior of folic acid: evidence for possible antioxidant activity. Free Radical Biology and Medicine 2001;30:1390-9.

Kanemitsu H, Yamauchi H, Komatsu M, Yamamoto S, Okazaki S, Nakayama H. Time-course changes in neural cell apoptosis in the rat fetal brain from dams treated with 6-mercaptopurine (6-MP). Histology and Histopathology 2009a;24:317-24.

Kanemitsu H, Yamauchi H, Komatsu M, Yamamoto S, Okazaki S, Uchida K, et al. 6-Mercaptopurine (6-MP) induces cell cycle arrest and apoptosis of neural progenitor cells in the developing fetal rat brain. Neurotoxicology and Teratology 2009b;31:104-9.

Katayama K, Ishigami N, Uetsuka K, Nakayama H, Doi K. Ethylnitrosourea (ENU)-induced apoptosis in the rat fetal tissues. Histology and Histopathology 2000;15:707-11.

Katayama K, Ueno M, Yamauchi H, Nagata T, Nakayama H, Doi K. Ethylnitrosourea induces neural progenitor cell apoptosis after S-phase accumulation in a

p53-dependent manner. Neurobiology of Disease 2005;18:218-25.

Katayama K, Uetsuka K, Ishigami N, Nakayama H, Doi K. Apoptotic cell death and cell proliferative activity in the rat fetal central nervous system from dams administered with ethylnitrosourea (ENU). Histology and Histopathology 2001;16:79-85.

Kobayashi K, Terada C, Tsukamoto I. Methotrexate-induced apoptosis in hepatocytes after partial hepatectomy. European Journal of Pharmacology 2002;438:19-24.

Komatsu K, Takada G, Uemura K, Shishido F, Kanno I. Decrease in cerebral metabolic rate of glucose after high-dose methotrexate in childhood acute lymphocytic leukemia. Pediatric Neurology 1990;6:303-6.

Kozma C, Ramasethu J. Methotrexate and misoprostol teratogenicity: further expansion of the clinical manifestations. American Journal of Medical Genetics. Part A 2011;155:1723-8.

Kremer JM, Phelps CT. Long-term prospective study of the use of methotrexate in the treatment of rheumatoid arthritis. Update after a mean of 90 months. Arthritis and Rheumatism 1992;35:138-45.

Kumar B, Handa S, Kaur I. Short term methotrexate therapy in psoriasis. The Indian Journal of Medical Research 1994;100:277-80.

Lipscomb GH. Medical therapy for ectopic pregnancy. Seminars in Reproductive Medicine 2007;25:93-8.

Lloyd ME, Carr M, McElhatton P, Hall GM, Hughes RA. The effects of methotrexate on pregnancy, fertility and lactation. QJM 1999;92:551-63.

Malassiné A, Frendo JL, Evain-Brion D. A comparison of placental development and endocrine functions between the human and mouse model. Human Reproduction Update 2003;9:531-9.

Margolis S, Philips FS, Sternberg SS. The cytotoxicity of methotrexate in mouse small intestine in relation to inhibition of folic acid reductase and of DNA synthesis. Cancer Research 1971;31:2037-46.

Martinez Lopez JA, Loza E, Carmona L. Systematic review on the safety of methotrexate in rheumatoid arthritis regarding the reproductive system (fertility, pregnancy, and breastfeeding). Clinical and Experimental Rheumatology 2009;27:678-84.

Müller M, Strand S, Hug H, Heinemann EM, Walczak H, Hofmann WJ, et al. Drug-induced apoptosis in hepatoma cells is mediated by the CD95 (APO-1/Fas) receptor/ligand system and involves activation of wild-type p53. The Journal of Clinical Investigation 1997;99:403-13.

Nam C, Woo GH, Uetsuka K, Nakayama H, Doi K. Histopathological changes in the brain of mouse fetuses by etoposide-administration. Histology and Histopathology 2006;21:257-63.

Ohira T, Ando R, Andoh R, Nakazawa T, Nishihara K, Yamamoto S, et al. Distribution and sequence of pyknotic cells in rat fetuses exposed to busulfan. Journal of Toxicologic Pathology 2009;22:167-71.

Ohira T, Ando R, Okada Y, Suzuki H, Saito T, Nakazawa T, et al. Sequence of busulfan-induced neural progenitor cell damage in the fetal rat brain. Experimental and Toxicologic Pathology 2013;65:523-30.

Passemard S, Kaindl AM, Verloes A. Microcephaly. Handbook of Clinical Neurology 2013;111:129-41.

Peel S, Bulmer D. Proliferation and differentiation of trophoblast in the establishment of the rat chorio-allantonic placenta. Journal of Anatomy 1977;124:675-87.

Pisarska MD, Carson SA, Buster JE. Ectopic pregnancy. Lancet 1998;351:1115-20.

Practice Committee of American Society for Reproductive Medicine. Medical treatment of ectopic pregnancy. Fertility and Sterility 2008;90:S206-12.

Sasaki K, Duan J, Murohara T, Ikeda H, Shintani S, Shimada T, et al. Rescue of hypercholesterolemia-related impairment of angiogenesis by oral folate

supplementation. Journal of the American College of Cardiology 2003;42:364-72.

Sehata S, Kiyosawa N, Makino T, Atsumi F, Ito K, Yamoto T, et al. Morphological and microarray analysis of T-2 toxin-induced rat fetal brain lesion. Food and Chemical Toxicology 2004;42:1727-36.

Seidahmed MZ, Shaheed MM, Abdulbasit OB, Al Dohami H, Babiker M, Abdullah MA, et al. A case of methotrexate embryopathy with holoprosencephaly, expanding the phenotype. Birth Defects Research. Part A, Clinical and Molecular Teratology 2006;76:138-42.

Skalko RG, Gold MP. Teratogenicity of methotrexate in mice. Teratology 1974;9:159-64.

Soares MJ. The prolactin and growth hormone families: pregnancy-specific hormones/cytokines at the maternal-fetal interface. Reproductive Biology and Endocrinology 2004;2:51-66.

Soares MJ, Chapman BM, Rasmussen CA, Dai G, Kamei T, Orwig KE. Differentiation of trophoblast endocrine cells. Placenta 1996;17:277-89.

Spurlock CF 3rd, Tossberg JT, Fuchs HA, Olsen NJ, Aune TM. Methotrexate increases expression of cell cycle checkpoint genes via JNK activation. Arthritis

Rheumatism 2012;64:1780-9.

Sun J, Sugiyama A, Inoue S, Takeuchi T, Takeuchi T, Furukawa S. Effect of methotrexate on rat placenta development. Experimental and Toxicologic Pathology 2013;65:995-1002.

Takano T, Akahori S, Takeuchi Y, Ohno M. Neuronal apoptosis and gray matter heterotopia in microcephaly produced by cytosine arabinoside in mice. Brain Research 2006;1089:55-66.

Tamura T, Picciano MF. Folate and human reproduction. American Journal of Clinical Nutrition 2006;83:993-1016.

Tsibangu K, Leroy F, Doumont-Meyvis M. Effects of amethopterin (methotrexate) on the evolution of pregnancy in rats. Toxicology 1975;4:65-73.

Ueno M, Katayama K, Nakayama H, Doi K. Mechanisms of 5-azacytidine (5AzC)-induced toxicity in the rat foetal brain. International Journal of Experimental Pathology 2002a;83:139-50.

Ueno M, Katayama K, Yasoshima A, Nakayama H, Doi K. 5-Azacytidine (5AzC)-induced histopathological changes in the central nervous system of rat fetuses. Experimental and Toxicologic Pathology. 2002b;54:91-6.

Wagner C. Biochemical role of folate in cellular metabolism. In: Bailey LB, editor.

Folate in health and disease. New York: Marcel Dekker, Inc.; 1995. p.23-42.

Watson ED, Cross JC. Development of structures and transport functions in the mouse placenta. Physiology (Bethesda) 2005;20:180-93.

Wen SW, Zhou J, Yang Q, Fraser W, Olatunbosun O, Walker M. Maternal exposure to folic acid antagonists and placenta-mediated adverse pregnancy outcomes. Canadian Medical Association Journal 2008;179:1263-8.

Williams PJ, Bulmer JN, Innes BA, Broughton Pipkin F. Possible roles for folic acid in the regulation of trophoblast invasion and placental development in normal early human pregnancy. Biology of Reproduction 2011;84:1148-53.

Wilson JG, Scott WJ, Ritter EJ, Fradkin R. Comparative distribution and embryotoxicity of methotrexate in pregnant rats and rhesus monkeys. Teratology 1979;19:71-80

Woo GH, Katayama K, Jung JY, Uetsuka K, Bak EJ, Nakayama H, et al. Hydroxyurea (HU)-induced apoptosis in the mouse fetal tissues. Histology and Histopathology 2003;18:387-92.

Wright JC, Prigot A, Wright B, Weintraub S, Wright LT. An evaluation of folic acid antagonists in adults with neoplastic diseases: a study of 93 patients with incurable neoplasms. Journal of the National Medical

Association 1951;43:211-40.

Yamaguchi Y, Aoki A, Fukunaga Y, Matsushima K, Ebata T, Ikeya M, et al. 5-fluorouracil-induced histopathological changes in the central nervous system of rat fetuses. Histology and Histopathology 2009;24:133-9.

Yamauchi H, Katayama K, Ueno M, Uetsuka K, Nakayama H, Doi K. Involvement of p53 in 1-beta-D-arabinofuranosylcytosine-induced rat fetal brain lesions. Neurotoxicology and Teratology 2004;26:579-86.

Zamenhof S. Differential effects of antifolate on the development of brain parts in chick embryos. Growth 1985;49:28-33.